Research Square

Preprints are preliminary reports that have not undergone peer review.
They should not be considered conclusive, used to inform clinical practice,
or referenced by the media as validated information.

Anti-inflammatory programming of macrophages by GDF-15 provides a beneficial effect for patients with clear cell renal cell carcinoma

Lina Susana Silva-Bermudez
Heidelberg University
Jingxuan Xu
Heidelberg University
Nil Aymat Alvarez
Heidelberg University
Jaroslava Zajakina
Heidelberg University
Christina Schmuttermaier
Heidelberg University
Ann-Katrin Niedermayer
Heidelberg University
Katja Nitschke
Heidelberg University
Thomas Worst
Heidelberg University
Bruno Reible
Heidelberg University
Christoph Brochhausen
Heidelberg University
Christel Weiss
Heidelberg University
Harald Klüter
Heidelberg University
Julia Kzhyshkowska
julia.kzhyshkowska@medma.uni-heidelberg.de

Heidelberg University

Research Article

Keywords: GDF-15, TGFBR1, macrophage, STAT6, Smad2/3, renal carcinoma

Posted Date: November 19th, 2026

DOI: https://doi.org/10.21203/rs.3.rs-11775287/v1

License: This work is licensed under a Creative Commons Attribution 4.0 International License.
Read Full License

Additional Declarations: No competing interests reported.

Anti-inflammatory programming of macrophages by GDF-15 provides a beneficial effect for patients with clear cell renal cell carcinoma

Lina S. Silva-Bermudez[1,2], Jingxuan Xu[1], Nil Aymat_Alvarez[1], Jaroslava Zajakina[1], Christina Schmuttermaier[1], Ann-Katrin Niedermayer[1], Katja Nitschke[3], Thomas Worst[3], Bruno Reible[4], Christoph Brochhausen[4], Christel Weiss[5], Harald Klüter[1,2], Julia Kzhyshkowska[1,2*]

[1]Institute of Transfusion Medicine and Immunology, Mannheim, Institute for Innate Immunoscience (MI3), Medical Faculty Mannheim, Heidelberg University, Mannheim, 68167, Germany

[2]German Red Cross Blood Service Baden-Württemberg – Hessen, Mannheim, 68167, Germany

[3]Department of Urology and Urosurgery, Medical Faculty Mannheim, Heidelberg University, Mannheim, 68167, Germany

[4]Institute of Pathology, Medical Faculty Mannheim, Heidelberg University, Mannheim, Germany

[5]Department of Medical Statistics and Biomathematics, Medical Faculty Mannheim, Heidelberg University, Mannheim, 68167, Germany

*Corresponding author at: Institute of Transfusion Medicine and Immunology, Mannheim Institute for Innate Immunoscience (MI3), Medical Faculty Mannheim, Heidelberg University, 68167, Germany, julia.kzhyskowska@medma.uni-heidelberg.de, 049 621 383 71716

Abstract

Background: Anti-GDF-15 antibody currently undergoes validation in clinical trials as a novel therapy for several solid cancers. Macrophages are key regulators of the tumor immune microenvironment and act as a source and target of GDF-15. GDF-15 effect on macrophage programming is an open question.

Methods: RNA sequencing (RNA seq) followed by RT-qPCR was used to identify the transcriptome induced by GDF-15 in primary human monocyte-derived macrophages. Western blotting was used to examine signaling pathways. Bioinformatic analysis of GDF15/IL17RB/IL8 pathway was performed using TCGA datasets. Tumor samples from 62 patients with primary clear cell renal cell carcinoma (ccRCC) who underwent nephrectomy between 2006 and 2011 were analyzed by RT-qPCR, immunohistochemistry and confocal microscopy.

Results: RNA seq showed that rGDF-15 treatment altered 210 genes in M0 and 372 in M2 (IL-4-driven) macrophages, with enrichment in angiogenesis and immune regulation pathways. GDF-15-target gene IL17RB was significantly upregulated and functionally responsive to its ligand IL-17E. Despite enhanced NF-κB p65 phosphorylation after stimulation with IL-17E, an IL17RB ligand, GDF-15 reduced IL-6 and IL-8 production, indicating an anti-inflammatory effect. Mechanistically, GDF-15 enhanced STAT6 and induced Smad2/3 phosphorylation, and both responses were abrogated by pharmacological inhibition of TGFBR1. TCGA analyses of ccRCC samples revealed that higher IL17RB expression was associated with favorable overall and disease-specific survival (DSS), whereas higher IL8 expression was associated with unfavorable survival outcomes. In an internal cohort of 62 patients with ccRCC, GDF15 correlated with IL17RB expression and remained independently associated with IL17RB after adjustment for clinicopathological variables. Confocal microscopy confirmed that IL17RB is almost exclusively expressed in CD68+ macrophages within

ccRCC tumors. Although neither GDF15 nor IL17RB was associated with DSS in the internal cohort, IL8 was associated with worse DSS in an exploratory multivariable analysis. The favorable association of IL17RB with survival in TCGA, together with its macrophage localization, supports the existence of a potentially protective GDF-15-associated state in ccRCC.

Conclusions: These findings suggest that broad GDF-15 blockade may have unfavorable consequences in selected ccRCC contexts and support tumor-specific evaluation of GDF-15-targeted therapies.

Key words

GDF-15; TGFBR1, macrophage; STAT6; Smad2/3, renal carcinoma

Plain English summary

GDF-15 is a blood biomarker best known for its role in appetite regulation and energy balance. In recent years, increased GDF-15 levels have also been linked to conditions associated with cellular stress, including myocardial infarction, infection, and cancer. More recently, attention has focused on its effects on the immune system and on strategies that block GDF-15 to improve cancer therapy. Macrophages are immune cells that rapidly respond to stress, infection, and tissue damage. They can produce GDF-15 but can also respond to it. In this study, we investigated how GDF-15 affects human macrophages by analyzing changes in gene expression after GDF-15 exposure. We then looked more closely at IL17RB, one of the genes increased by GDF-15. Our results suggest that GDF-15 reduces inflammatory signals such as IL-8, through IL17RB engagement. We also studied whether these findings might be relevant in clear cell renal cell carcinoma, the most common type of kidney cancer. In a large kidney cancer dataset, patients with higher IL17RB levels tended to have better outcomes, whereas higher IL-8 levels were linked to worse outcomes. Together with

our macrophage experiments, these findings suggest that GDF-15 may influence the tumor environment in ways that differ between cancer types. Therefore, blocking GDF-15 may not have the same effect in every cancer, and its effects in clear cell renal cell carcinoma should be studied carefully.

Background

Growth differentiation factor 15 (GDF-15), also known as macrophage-inhibiting cytokine-1 (MIC-1), is a multifunctional cytokine recognized as a distant member of the glial cell-derived neurotrophic factor (GDNF) family and the transforming growth factor-β (TGF-β) superfamily [1]. Elevated GDF-15 levels are observed in sepsis, cardiometabolic disorders, and cancer, often correlating with disease severity and survival [2]. In neuronal cells, GDF-15 signals through its receptor GDNF family receptor α-like (GFRAL) in the area postrema and nucleus of the solitary tract in the brain, triggering nausea and reduced energy intake, and is currently being investigated as a therapeutic target for cachexia, a syndrome characterized by anorexia, skeletal muscle loss, and weakness in chronic disease [1, 3-5]. GDF-15 has also been implicated in tumor biology, with preclinical and clinical evidence suggesting a pro-tumorigenic function [6-9]. For the majority of tumor types, including colorectal, pancreatic, breast, and prostate cancers, GDF-15 levels correlate with poor prognosis, immune evasion, and chemoresistance, where GDF-15-mediated modulation of fatty acid metabolism, epithelial-mesenchymal transition, and suppression of anti-tumor immunity were recently summarized as key pro-tumoral mechanisms [10]. The immunosuppressive mechanisms are primarily attributed to the impaired dendritic cell (DC) maturation and suppressed $CD8^+$ T-cell infiltration [10].

However, the effects of GDF-15 are not uniform across cellular and tumor contexts. Recent experimental evidence suggests that macrophage-derived GDF-15 may support phagocytosis, antigen cross-presentation, and $CD8^+$ T-cell recruitment in selected tumor models, contrasting with the immunosuppressive effects attributed to tumor-derived or circulating GDF-15 [11]. This context dependence may be particularly relevant in clear cell renal cell carcinoma (ccRCC), where the clinical significance of

$CD8^+$ T-cell infiltration is complex and specific dysfunctional or exhausted $CD8^+$ populations have been associated with unfavorable outcomes [12]. Moreover, the molecular mechanisms by which GDF-15 acts, particularly within the tumor-specific immune microenvironment, remain insufficiently understood and require deep investigation to guide therapeutic strategies [13]. This is particularly relevant given the clinical development of GDF-15-neutralizing antibodies in combination with immune checkpoint inhibitors, initially to overcome resistance to anti-programmed cell death protein 1 (PD-1) or anti-programmed death-ligand 1 (PD-L1) therapies in advanced solid tumors and subsequently in immunotherapy-naïve settings [14-17]. More recently, GDF-15 neutralization has also entered clinical evaluation in combination with standard chemoimmunotherapy for metastatic non-small cell lung cancer and unresectable or metastatic hepatocellular carcinoma (NCT07098988, NCT07246863).

Macrophages are essential innate immune cells for both inflammatory and healing processes. In most solid cancers, macrophages promote tumor initiation and progression [18]. They support cancer cell proliferation, induce tumor angiogenesis and intratumoral matrix remodeling, create a low-grade inflammatory environment, and suppress cytotoxic adaptive immune responses [18-20]. The pro-tumoral activity of tumor-associated macrophages (TAMs) is actively programmed by cancer cells at the metabolic, transcriptional, and epigenetic levels [21, 22]. It has recently been recognized that pro-tumoral TAMs are a major obstacle to the effectiveness of immune checkpoint inhibitors and chimeric antigen receptor (CAR)-T-cell therapies against solid tumors [20, 23, 24].

Macrophages are identified both as a source and a target of GDF-15 [2]. Under stress conditions, macrophages secrete higher levels of GDF-15, thereby contributing to circulating GDF-15 levels [25, 26]. TAMs have also been shown to produce GDF-15 in

several cancer types, such as acute myeloid leukemia, gastric, colorectal, and esophageal squamous cell carcinoma [7, 8, 27, 28]. As a macrophage-targeting factor, GDF-15 induces an anti-inflammatory phenotype by promoting M2 and inhibiting M1-like phenotypes in in vitro and in animal models [25, 29, 30]. However, limited attention has been paid to the molecular mechanisms underlying GDF-15 direct effects on macrophage programming. Moreover, the concept of M1/M2 dichotomy in vivo, including in the tumor microenvironment, was recently substantially revised due to the high variability and diversity of macrophage subpopulations, defined by their origin and local programming factors [31, 32].

Given the importance of macrophages in the tumor microenvironment and the growing therapeutic potential of GDF-15 in cancer, we aimed to identify the transcriptional program induced by GDF-15 in human macrophages. Here, we report for the first time that GDF-15 induces significant transcriptional changes in primary human macrophages. We focused on the GDF-15-upregulated interleukin-17 receptor β (IL17RB), examined how GDF-15 utilizes two anti-inflammatory signaling pathways affecting the outcome of IL17RB signaling and inflammatory cytokine production. Finally, we explored the relevance of this pathway in ccRCC. In our institutional cohort, GDF15 expression was positively associated with IL17RB expression, and IL17RB was predominantly localized to $CD68^{+}$ macrophages within tumor tissue. In The Cancer Genome Atlas (TCGA) ccRCC cohort, higher IL17RB expression was associated with favorable overall (OS) and disease-specific survival (DSS). Together, these observations suggest that IL17RB may mark a macrophage-associated regulatory program with potential clinical relevance in ccRCC.

Methods

Patient description

We retrospectively analyzed clinicopathological data from 62 patients with primary ccRCC who underwent partial or radical nephrectomy in the Department of Urology and Urosurgery of the Mannheim Medical Center between 2006 and 2011. The study was approved by the institutional ethics committee (ethics approval 2015-549N-MA and 2024-591-MA). Written informed consent was obtained from all participants. Tissue samples were stored for RNA extraction for RT-qPCR and immunohistochemistry, as described below.

Primary human monocyte isolation and generation of macrophages

Monocytes were isolated from buffy coats of healthy blood donors (German Red Cross Blood Service Baden-Württemberg – Hessen) after informed consent, as previously described [33]. CD14+ monocytes were isolated using sequential density gradient centrifugation and CD14+ magnetic-activated cell sorting (MACS) (Miltenyi Biotech, Bergisch Gladbach, Germany), resulting in 90-98% monocyte purity, as verified by flow cytometry. Cells were seeded at 1 x 10^6 cells/mL in custom serum-free medium (SFM, Gibco, Germany) supplemented with 5 mM glucose. Differentiation into macrophages was induced with macrophage colony-stimulating factor (M-CSF) at 5 ng/mL (Peprotech, Hamburg, Germany) and dexamethasone 10^{-8} M (Sigma Aldrich, Darmstadt, Germany). For polarization, IFN-γ (100 ng/mL) was added for M1 and IL-4 (10 ng/mL) for M2 macrophages (Peprotech, Hamburg, Germany). No cytokines were added for M0 differentiation. Conditioned medium was harvested for enzyme-linked immunosorbent assay (ELISA) and cells were harvested for flow cytometry, Western blot analysis, RNA isolation, RT-qPCR, and RNA sequencing (RNA seq).

Stimulation with rGDF-15

Differentiated macrophages were cultured in the presence or absence of recombinant human GDF-15 (rGDF-15) (Peprotech, Hamburg, Germany) at 10-100 ng/mL, according to the following experimental designs: model 1: 48-h rGDF-15 treatment on day 6 of differentiation; model 2: continuous rGDF-15 exposure during the 6-day differentiation; model 3: 1-h rGDF-15 treatment on day 6. Following rGDF-15 treatment, cells were stimulated with lipopolysaccharide (LPS) 100 ng/mL (Sigma-Aldrich, Darmstadt, Germany) for 6 h. For the RNA seq analysis, M0 or M2 were incubated with or without 50 ng/mL rGDF-15 for 7 h. To assess the persistence of rGDF-15 effect on macrophages, M2 were treated with or without rGDF-15 for 0-96 h. For the Western blot analysis, M2 were treated with or without rGDF-15 for 24 h, followed by incubation with 100 ng/mL recombinant IL-17E (R&D Systems, Minneapolis, United States) for 10-60 min. For the cytokine expression analysis, M2 were treated with or without 50 ng/mL rGDF-15 for 24 h, followed by a 6- or 24-h incubation in the presence or absence of 100 ng/mL IL-17E.

RT-qPCR

Total RNA was isolated from macrophages using the E.Z.N.A. Total RNA kit I (Omega Bio-tek, Norcross, USA) according to the manufacturer's instructions. For patient tissue, RNA was isolated using the magnetic bead-based XTRAKT FFPE kit (Stratifyer, Cologne, Germany). RNA was reverse transcribed using the SensiFAST cDNA Synthesis Kit (Bioline, Luckenwalde, Germany). Diluted cDNA was amplified using SensiMixTM II Probe No-ROX Kit Bioline, Luckenwalde, Germany) in an RT-qPCR cycler using the ready-to-use TaqMan master mixes containing probes for GDF-15 (Hs00171132_m1), IL17RB (Hs00218889_m1), C-X-C motif chemokine ligand 8 (CXCL8) (Hs00174103_m1), IL6 (Hs00174131_m1) and CD68 (Hs02836816_g1). Additional primers are listed in Table 1 (5′→3′ orientation) (Eurofins, Ebersberg,

Germany). Target gene expression data were normalized to 18S as an endogenous control. Duplicates were performed for each sample. For the RT-qPCR performed on patient tissue ccRCC samples, relative expression was calculated using the 2-ΔΔCT method, with one tumor sample serving as the reference (fold change = 1).

Table 1. List of primers purchased from Eurofins

Target Gene	Primer name	Sequence (5'-3' direction)
18SrRNA	FP2242	CCATTCGAACGTCTGCCCTAT
	RP2242	TCACCCGTGGTCACCATG
	Pr2242	ACTTTCGATGGTAGTCGCCGTGCCT
TNF-α	F896	TCTTCTCGAACCCCGAGTGA
	R896	AGCTGCCCCTCAGCTTGA
	Pr896	AAGCCTGTAGCCCATGTTGTAGCAAACC

F: forward, Pr: probe, R: reverse, rRNA: ribosomal RNA, TNF-α: tumor necrosis factor alpha

RNA sequencing and bioinformatics analysis

Total RNA from rGDF-15-treated M0 and M2 cells and controls was extracted using the RNeasy Mini Kit (Qiagen, Hilden, Germany). RNA quantity was measured with a NanoDrop® spectrophotometer, and integrity was verified by agarose gel electrophoresis. Samples with >300 ng RNA were submitted to Novogene (Cambridge, United Kingdom) for sequencing. Poly(A) mRNA was enriched with oligo(dT) magnetic beads, and cDNA libraries were prepared using the SMART™ PCR cDNA Synthesis Kit. Sequencing was performed on an Illumina HiScanSQ platform, yielding approximately 20 million reads per sample. Differential expression analysis was conducted with DESeq2, using $|\text{Log2(FoldChange)}| > 1$ and adjusted p-value < 0.05 (Benjamini–Hochberg correction) as significance thresholds. Results were visualized

as volcano plots, and functional enrichment was assessed by Gene Ontology (GO) analysis using the clusterProfiler R package, with figures generated in GraphPad Prism 10.4.

Cytokine secretion assay

IL-8 concentrations in macrophage culture supernatants were measured by ELISA (R&D Systems, Wiesbaden, Germany) according to the manufacturer's protocol.

Flow cytometry

IL17RB expression was quantified by flow cytometry in permeabilized macrophages. Cells were fixed with 4% paraformaldehyde, permeabilized with 0.1% saponin, and blocked with FcR reagent (Miltenyi Biotec, Bergisch Gladbach, Germany). Cells were stained with APC-conjugated human anti-IL17RB or isotype control antibodies (R&D Systems, USA). Fluorescent signal was quantified using a BD FACS Canto II flow cytometer at the core facility FlowCore of the Medical Faculty Mannheim at Heidelberg University. The data were analyzed using FlowJo 10.01 software.

Western blot analysis of signal transduction

Cells were lysed with RIPA buffer containing protease and phosphatase inhibitors (Roche, Mannheim, Germany). Lysates were cleared by centrifugation and mixed with Laemmli buffer, boiled, separated by SDS-PAGE, and transferred to membranes. Membranes were blocked (5% non-fat milk in TBST) and incubated overnight at 4°C with primary antibodies against phospho-p38 mitogen-activated protein kinase (MAPK), p38MAPK, phospho-NF-κB p65, NF-κBp65, STAT6, p-STAT6, SMAD2/3, p-SMAD2/3 (all from Cell Signaling Technology), and β-actin (Proteintech) (all diluted in 5% BSA/TBST). Horseradish peroxidase (HRP)-conjugated secondary antibodies

were applied, and signals were visualized using a ChemiDoc Imaging System (Biorad, California, United States). For the TGFBR1 inhibition assay, the selective inhibitor HY-12043 (SB-525334) (Hycultec, Beutelsbach, Germany) was used at a concentration of 1 µM to pretreat macrophages for 1 hour before the stimulation with rGDF-15.

Immunohistochemistry

After deparaffinization of paraffin-embedded tumor tissue sections, heat-induced antigen retrieval (HIER) in Tris-EDTA buffer (pH 9.0) (Zytomed Systems, Berlin, Germany) was performed. After antigen retrieval, endogenous peroxidase activity was quenched with 0.3% H_2O_2. Sections were blocked with 3% BSA/PBS and incubated with one of the following primary antibodies: rabbit anti-human IL17RB (1:400, Proteintech, Planegg-Martinsried, Germany), mouse anti-human GDF-15 (1:400, Atlas Antibodies, Stockholm, Sweden), mouse anti-human CD68 monoclonal antibody (1:100, Thermofisher, Darmstadt, Germany) or isotype control (purified mouse IgG1, κ: 1:100, BD Biosciences, Heidelberg, Germany, or rabbit IgG polyclonal antibody: 1:400, Merck, Darmstadt, Germany). A matching secondary antibody, HRP-labeled anti-mouse antibody (EnVision+ kit, Dako, Agilent, Waldbronn, Germany) or HRP-labeled anti-rabbit antibody (OriGene, Herford, Germany) was used. The HRP enzyme was developed with AEC chromogen (Zytomed Systems, Berlin, Germany) to yield a visible red reaction product, and sections were then counterstained with Mayer's hemalum solution (Merck, Darmstadt, Germany). Slides were analyzed using a Leica upright light microscope DMRE (Core Facility Live Cell Imaging Mannheim, Medical Faculty Mannheim, Heidelberg University).

Immunofluorescent staining and confocal microscopy

Following deparaffinization and antigen retrieval as above, sections were co-stained with mouse monoclonal anti-human CD68 (1:500, Thermofisher, Darmstadt, Germany) and rabbit polyclonal anti-human IL17RB (1:800, Proteintech, Planegg-Martinsried, Germany). As isotype controls purified mouse IgG1, κ, (1:500, BD Biosciences, Heidelberg, Germany) or rabbit IgG polyclonal antibody (1:800, Proteintech, Planegg-Martinsried, Germany) were used. Secondary antibodies were Cy3-conjugated donkey anti-rabbit IgG (1:400, Dianova, Hamburg, Germany) and an AlexaFluor488-conjugated donkey anti-mouse IgG (1:400, Dianova, Hamburg, Germany). For the nuclear translocation assessment, macrophages were visualized after 30 min or 1 h of stimulation with recombinant IL17E (R&D Systems, Minneapolis, United States) or tumor necrosis factor alpha (TNF-α) (PreproTech, New Jersey, United States). NF-κB p65 translocation was assessed using an anti-NF-κB p65 (D14E12) rabbit monoclonal antibody (Cell Signalling Techology, Massachusetts, United States). Nuclei were counterstained with DAPI (1:1000, Roche, Mannheim, Germany). Confocal microscopy was performed on a Leica TCS SP8 upright laser-scanning microscope equipped with a 40× oil objective under sequential scanning (Leica Microsystems, Wetzlar, Germany). Excitation was performed using laser lines at 405 nm, 488 nm, and 552 nm. Images were acquired using the Leica Confocal software, version 2.5 (Leica Microsystems, Wetzlar, Germany). Images were assembled into final panels using Adobe Photoshop, version CC2017 (Adobe Systems, San Jose, CA). Confocal imaging was performed at the LIMA core facility (Medical Faculty Mannheim, Heidelberg University).

Pan-cancer analysis

Gene expression profiles (RNA seq) and clinical data for the ccRCC cohort were retrieved from TCGA via the UCSC Xena platform [34]. The association between

mRNA levels of GDF-15, IL17RB, and IL8 and clinical parameters was analyzed. Analysis of CD8+ T cell infiltration and GDF15 expression in patients with ccRCC (TCGA) using the Tumor Immune Estimation Resource (TIMER) [35].

Statistical analysis

Normality was assessed with the Shapiro–Wilk test. For two-group comparisons, Student's paired t-test (normally distributed) or Wilcoxon matched-pairs rank test (non-normal) was applied. Fold-change differences from RT-qPCR were analyzed using the ratio paired t-test. Categorical data were analyzed by Fisher's exact test. Survival was evaluated by the log-rank (Mantel–Cox) test. Correlations were assessed by Spearman's rank test. All statistical analyses were generated using GraphPad Prism 10.4. A two-tailed p-value of less than 0.05 was considered to indicate statistical significance (confidence level 95%). Significance is reported as ns (not significant), *p<0.05, **p≤0.01, ***p≤0.001, ****p≤0.0001.

Data availability

The original RNA seq data for all differentially activated genes is available on the NCBI Gene Expression Omnibus (GEO) browser (Reference number GSE308883).

Results

rGDF-15 reduces the inflammatory response of macrophages to LPS

To explore the role of GDF-15 in macrophage programming, we first evaluated the effect of rGDF-15 on the inflammatory responses of primary human monocyte-derived macrophages to LPS, as a prototype pro-inflammatory stimulus. Macrophages were differentiated for 6 days and exposed to varying concentrations of rGDF-15 (10 to 100

ng/mL) at different time points. After rGDF-15 treatment, cells were challenged with LPS for 6 h, according to the experimental design. In model 1, macrophages were incubated with rGDF-15 for 48 h (Fig.1A, B). In model 2, rGDF-15 was added to the medium during plating (day 0) (Fig.1C, D). Finally, model 3 included a 1 h treatment with rGDF-15 (Fig. 1E, F). TNF-α was selected as a reference gene for the acute inflammatory response and its expression was analyzed by RT-qPCR in homeostatic M0, acute inflammatory M1, and healing M2 macrophages (Fig. 1). rGDF-15 alone did not alter TNF-α expression compared with untreated controls, regardless of rGDF-15 concentration. As expected, LPS stimulation markedly increased TNF-α expression in all models compared with non-LPS-stimulated conditions. However, this effect only reached statistical significance in models 1 and 3 (Model 1: p=0.0313 for M0, p=0.0156 for M1, and p=0.0313 for M2; Model 2: p=0.2162 for M0, p=0.2319 for M1, and p=0.1809 for M2; Model 3: p=0.0016 for M0, p=0.1250 for M1, and p=0.0020 for M2). In model 1, TNF-α expression was significantly downregulated in M0 and M1 treated with high doses of rGDF-15 (GDF-15 100 ng/mL + LPS vs LPS p=0.0313 for M0 and p=0.0156 for M1) (Fig. 1B). Although not statistically significant, a dose-response trend was evident, particularly in M0 and M1 in the models 1 and 2 (Figs. 1B, D). The most pronounced effect of rGDF-15 on TNF-α expression was demonstrated in model 3 with 1 h exposure to rGDF-15. In this model, TNF-α expression was significantly reduced in M0 and M2 macrophages after LPS challenge, even at lower rGDF-15 concentrations. This was the case in M0 pre-exposed to 50 ng/mL (p=0.0391) and in M2 pre-exposed to 10, 25, 50, and 100 ng/mL rGDF-15 (p=0.0194; p=0.0332, p=0.0083, and p=0.0088, respectively) (Fig. 1F).

All three models demonstrated a direct inhibitory effect of rGDF-15 on TNF-α expression, indicating that GDF-15 tolerogenically programs primary human monocyte-derived macrophages. For whole-transcriptome profiling, we selected model

3 and performed RNA seq on M0 and M2 macrophages, which serve as prototypes of tolerogenic macrophages in the tumor microenvironment. We selected a dose of 50 ng/mL rGDF-15 and focused solely on its effect on macrophages, excluding the LPS challenge.

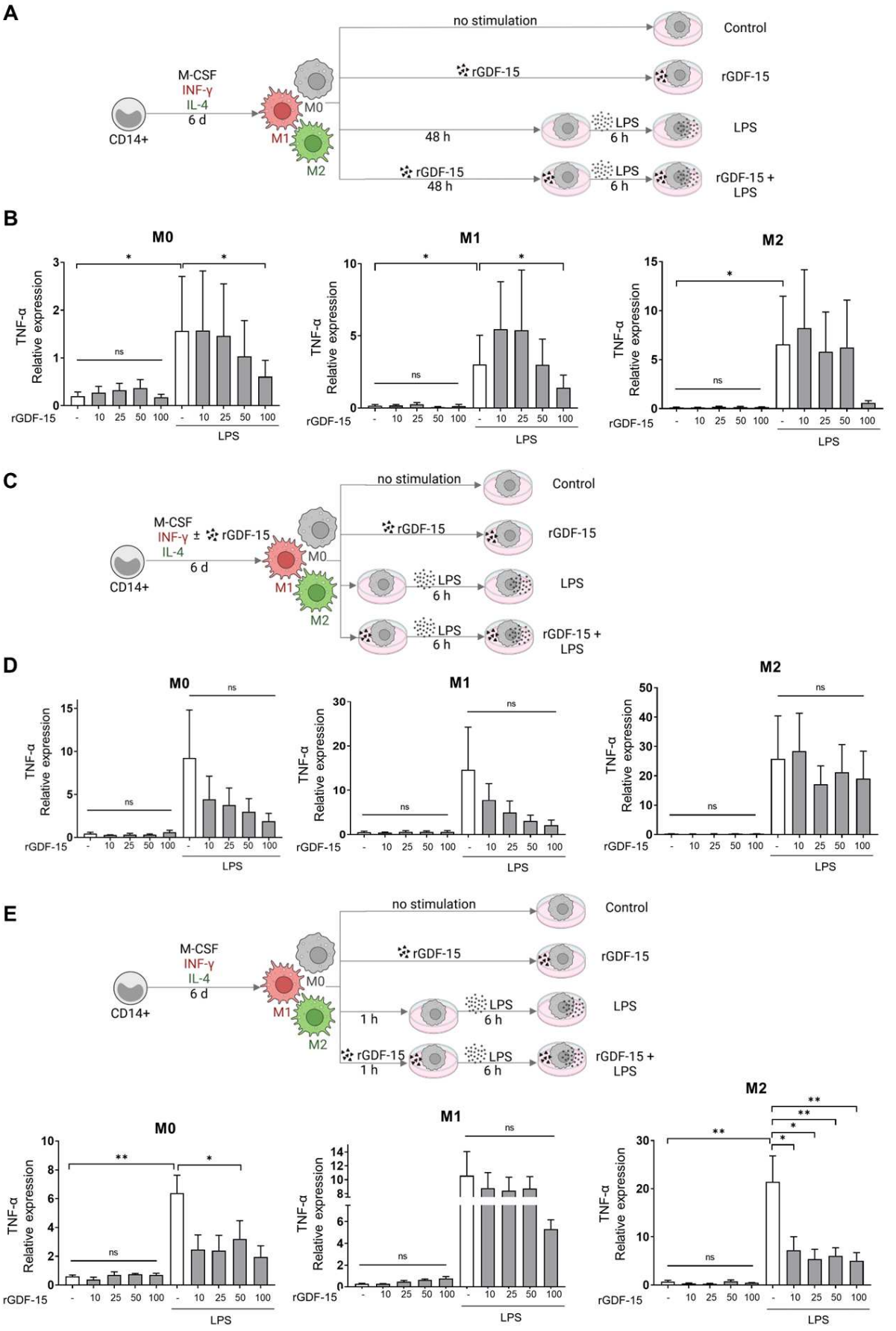
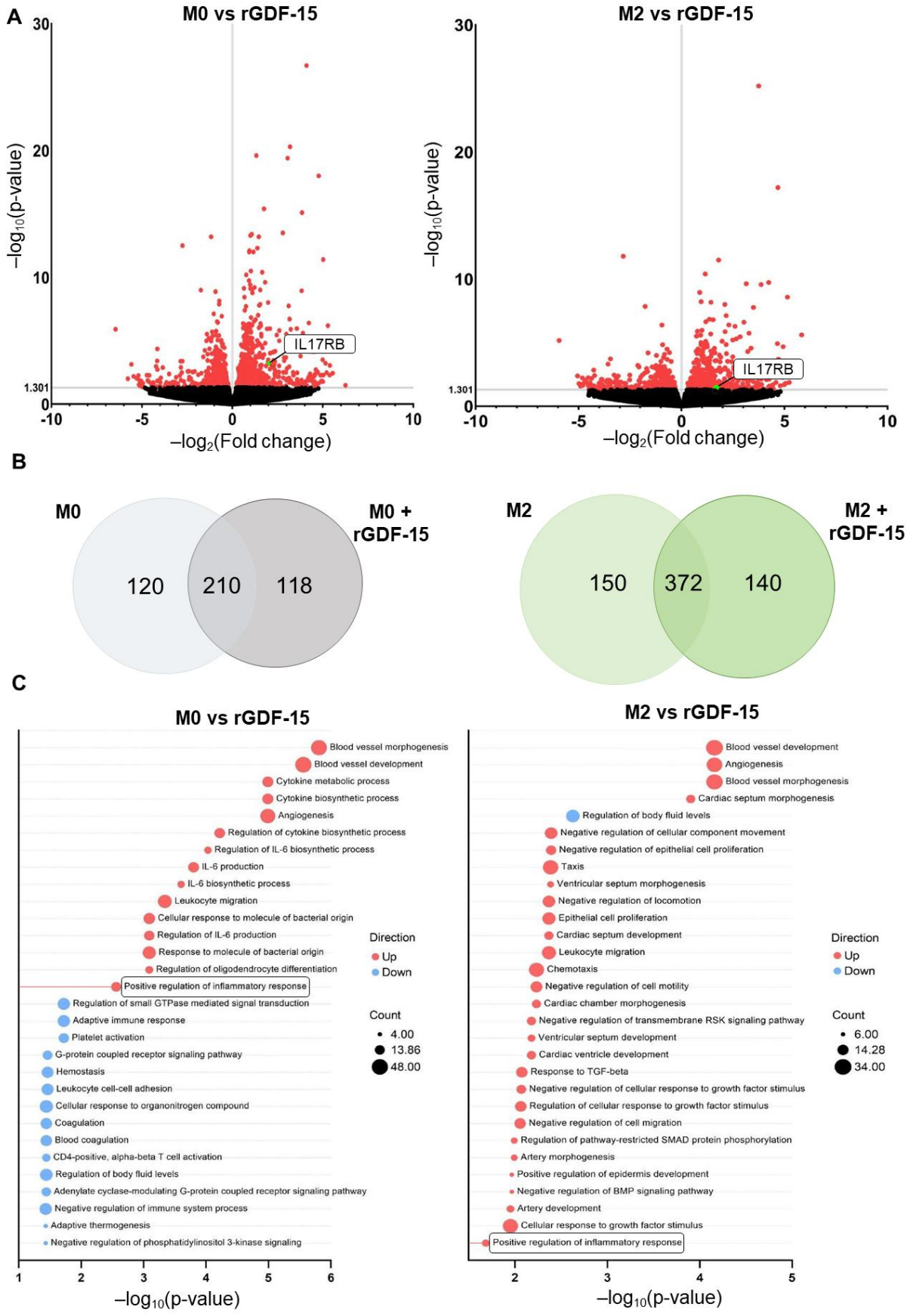


Fig. 1. rGDF-15 reduces LPS-induced TNF-α expression in M0, M1, and M2

macrophages. Monocytes were cultured and differentiated into M0 (non-stimulated, in gray), M1 (IFN-γ-stimulated, in red) and M2 (IL-4-stimulated, in green) for 6 days. rGDF-15 was tested at varying concentrations (10, 25, 50 and 100 ng/mL). LPS challenge consisted of a 6-h incubation with 100 ng/mL LPS. **A)** Schematic illustration of model 1. In model 1, rGDF-15 was added for 48 h on day 6, followed by the LPS challenge. **B)** TNF-α expression in model 1 assessed by RT-qPCR (n=4-7). **C)** Schematic illustration of model 2. In model 2, rGDF-15 was added after monocyte isolation. LPS challenge was performed on day 6. **D)** TNF-α expression in model 2 assessed by RT-qPCR (n=2-4). **E)** Schematic illustration of model 3. In model 3, rGDF-15 was added for 1 h on day 6, followed by the LPS challenge. **F)** TNF-α expression in model 3 assessed by RT-qPCR (n=3-9). Data are presented as mean ± SEM normalized to 18SrRNA expression levels. *p<0.05, **p<0.01. Schematic illustrations were Created in BioRender. Silva, L. (2027) https://BioRender.com/5t8bf7g.

Effect of rGDF-15 on the transcriptome of primary human monocyte-derived macrophages

We compared the transcriptomes of human monocyte-derived M0 and M2 macrophages, with or without rGDF-15 treatment (n=5 per group). Differential gene expression analysis revealed 526 upregulated and 674 downregulated genes in M0 vs. M0 + rGDF-15 and 342 upregulated and 461 downregulated genes in M2 vs. M2 + rGDF-15 (Fig. 2A). Using a threshold of fragments per kilobase of transcript per million (fpkm) >1, we identified 118 unique differentially expressed genes in M0 and 140 in M2, with 46.8% and 56.2% overlap between treated and untreated groups, respectively (Fig. 2B).

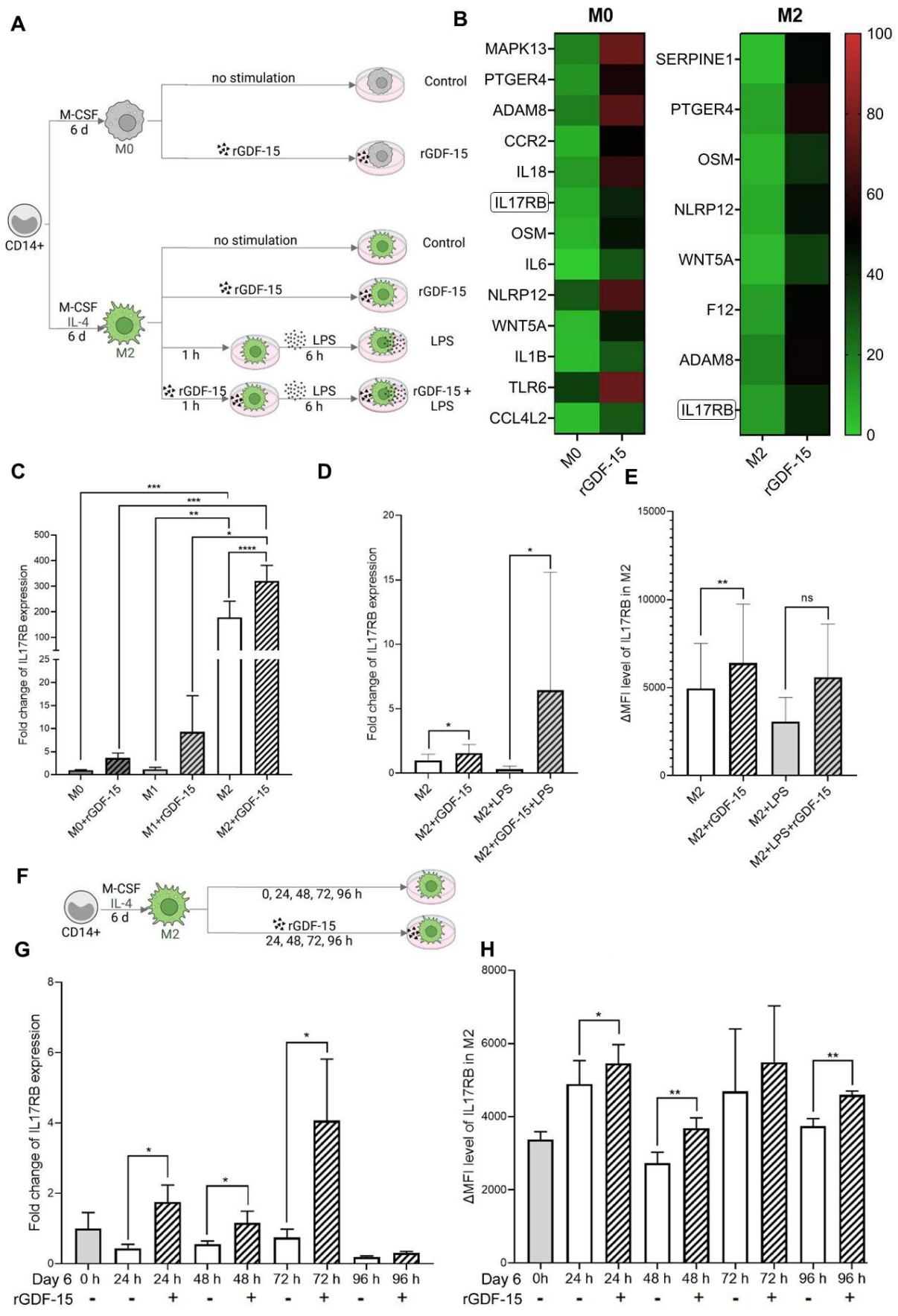

A
M0 vs rGDF-15
M2 vs rGDF-15
IL17RB
IL17RB
–log10(p-value)
–log2(Fold change)
B
M0
M0 + rGDF-15
120
210
118
M2
M2 + rGDF-15
150
372
140
C
M0 vs rGDF-15
M2 vs rGDF-15
Blood vessel morphogenesis
Blood vessel development
Cytokine metabolic process
Cytokine biosynthetic process
Angiogenesis
Regulation of cytokine biosynthetic process
Regulation of IL-6 biosynthetic process
IL-6 production
IL-6 biosynthetic process
Leukocyte migration
Cellular response to molecule of bacterial origin
Regulation of IL-6 production
Response to molecule of bacterial origin
Regulation of oligodendrocyte differentiation
Positive regulation of inflammatory response
Regulation of small GTPase mediated signal transduction
Adaptive immune response
Platelet activation
G-protein coupled receptor signaling pathway
Hemostasis
Leukocyte cell-cell adhesion
Cellular response to organonitrogen compound
Coagulation
Blood coagulation
CD4-positive, alpha-beta T cell activation
Regulation of body fluid levels
Adenylate cyclase-modulating G-protein coupled receptor signaling pathway
Negative regulation of immune system process
Adaptive thermogenesis
Negative regulation of phosphatidylinositol 3-kinase signaling
Direction
Up
Down
Count
4.00
13.86
48.00
–log10(p-value)
Blood vessel development
Angiogenesis
Blood vessel morphogenesis
Cardiac septum morphogenesis
Regulation of body fluid levels
Negative regulation of cellular component movement
Negative regulation of epithelial cell proliferation
Taxis
Ventricular septum morphogenesis
Negative regulation of locomotion
Epithelial cell proliferation
Cardiac septum development
Leukocyte migration
Chemotaxis
Negative regulation of cell motility
Cardiac chamber morphogenesis
Negative regulation of transmembrane RSK signaling pathway
Ventricular septum development
Cardiac ventricle development
Response to TGF-beta
Negative regulation of cellular response to growth factor stimulus
Regulation of cellular response to growth factor stimulus
Negative regulation of cell migration
Regulation of pathway-restricted SMAD protein phosphorylation
Artery morphogenesis
Positive regulation of epidermis development
Negative regulation of BMP signaling pathway
Artery development
Cellular response to growth factor stimulus
Positive regulation of inflammatory response
Direction
Up
Down
Count
6.00
14.28
34.00
–log10(p-value)

390

Fig. 2. Transcriptomic profiling of rGDF-15-treated macrophages. A) Volcano plots of differential expression analysis comparing rGDF-15-treated vs. untreated M0 (left) and untreated M2 (right). The X-axis is the log2 fold change of gene expression levels, while the Y-axis indicates the p-value based on -log10. Red color indicates up- or downregulated genes with a false discovery rate (FDR) less than 0.05. Black dots indicate non-differentially expressed (FDR > 0.05). The grey line shows the threshold for differential gene screening. **B)** Venn diagram intersection between the effects of rGDF-15 and control conditions in M0 and M2 (p-value < 0.05, fpkm > 1). **C)** Dot plots of the top 30 significant Gene Ontology (GO) pathways. To the left, the comparison M0 vs. M0 + rGDF-15. To the right, the comparison M2 vs. M2 + rGDF-15. Dot size represents the enriched gene count. Blue represents downregulated and red upregulated pathways. Significance is indicated by the adjusted p-value based on -log10 on the X-axis.

GO enrichment pathway analyses were used to assess specific terms enhanced by rGDF-15 (Fig. 2C). The two analyzed macrophage phenotypes shared several enriched pathways under the rGDF-15 stimulation. For instance, rGDF-15 treatment strongly enhanced pathways associated with angiogenesis and vascular remodeling (blood vessel morphogenesis, blood vessel development, regulation of angiogenesis, artery morphogenesis, artery development, regulation of vasculature development) as well as pathways related to the response to TGF-β (cellular response to TGF-β stimulus). Top enriched GO terms also highlighted a strong inflammation-related signature, such as in the upregulation of leukocyte migration, chemotaxis, and positive regulation of inflammatory response (Fig. 2C). Particularly in M0, rGDF-15 upregulated pathways linked to innate immune activation via toll-like receptor (TLR) and LPS signaling, IL-6 regulation, and response to bacterial molecules, while downregulating pathways related to hemostasis, platelet activation, leukocyte adhesion, and integrin binding. Interestingly, rGDF-15 provides an adaptive immunity-suppressive signature

418 in M0, downregulating pathways associated with $CD4^+$ T-cell activation and
419 differentiation. In M2, there were uniquely enriched SMAD phosphorylation pathways,
420 consistent with its enhancement of TGF-β signaling. In conclusion, rGDF-15 was
421 shown to be involved in important biological processes related to inflammation, tissue
422 remodeling, and angiogenesis in the macrophage system. All these processes play a
423 key role in tissue regeneration and are major hallmarks of cancer.
424
425 **rGDF-15 upregulates expression of IL17RB in macrophages**
426 Among the GO terms enriched in both M0 and M2 macrophages treated with rGDF-
427 15, “positive regulation of inflammatory response” was notably represented, with 13
428 and 8 significantly upregulated genes in M0 and M2, respectively (Fig. 3A, B). One key
429 gene was IL17RB, which was consistently upregulated in both phenotypes. IL17RB is
430 the receptor for IL-17E (IL-25) and signals via NF-κB and MAPK to induce
431 proinflammatory mediators such as IL-6 and IL-8 [36-40]. Given the reported
432 involvement of IL-17RB-mediated signaling in cancer progression and its potential as
433 a therapeutic target [41], we further investigated the functional significance of GDF-15-
434 induced IL17RB expression in macrophages.


A
CD14+
M-CSF
6 d
M0
no stimulation
Control
rGDF-15
rGDF-15
M-CSF
IL-4
6 d
M2
no stimulation
Control
rGDF-15
rGDF-15
1 h
LPS
6 h
LPS
rGDF-15
1 h
LPS
6 h
rGDF-15 + LPS
B
M0
M2
MAPK13
PTGER4
ADAM8
CCR2
IL18
IL17RB
OSM
IL6
NLRP12
WNT5A
IL1B
TLR6
CCL4L2
SERPINE1
PTGER4
OSM
NLRP12
WNT5A
F12
ADAM8
IL17RB
100
80
60
40
20
0
M0
rGDF-15
M2
rGDF-15
C
Fold change of IL17RB expression
M0
M0+rGDF-15
M1
M1+rGDF-15
M2
M2+rGDF-15
D
Fold change of IL17RB expression
M2
M2+rGDF-15
M2+LPS
M2+rGDF-15+LPS
E
ΔMFI level of IL17RB in M2
ns
M2
M2+rGDF-15
M2+LPS
M2+LPS+rGDF-15
F
CD14+
M-CSF
IL-4
6 d
M2
0, 24, 48, 72, 96 h
rGDF-15
24, 48, 72, 96 h
G
Fold change of IL17RB expression
Day 6 0 h 24 h 24 h 48 h 48 h 72 h 72 h 96 h 96 h
rGDF-15 - - + - + - + - +
H
ΔMFI level of IL17RB in M2
Day 6 0h 24 h 24 h 48 h 48 h 72 h 72 h 96 h 96 h
rGDF-15 - - + - + - + - +

435

Fig. 3. Effect of rGDF-15 on IL17RB expression in macrophages. A) Experimental design for rGDF-15 treatment on monocyte-derived macrophages. Monocytes were cultured and differentiated into M0 (non-stimulated, in grey) and M2 (IL-4-stimulated, in green) macrophages for 6 days, and then treated with ± 50 ng/mL rGDF-15, followed by RNA seq. For RT-qPCR validation, an inflammatory challenge with LPS (100 ng/mL, 6 h) was included. **B)** Heatmap of normalized enrichment score (NES) for upregulated genes enriched for the GO term "positive regulation of inflammatory response" across five replicates per group. Green represents relative downregulation and red upregulation **C)** RT-qPCR validation of IL17RB in M0, M1 and M2 (n=5). **D)** RT-qPCR for M2 primed with rGDF-15 and challenged with LPS (n=3). **E)** Flow cytometry analysis of IL17RB protein expression in M2 challenged with LPS (100 ng/mL, 24 h) (n=6). **F)** Experimental design to investigate the effects of rGDF-15 on sustained IL17RB gene and protein expression in M2 at indicated time points: 0, 24, 48, 72, 96 h following stimulation ± 50 ng/mL rGDF-15. **G)** IL17RB expression over time was assessed by RT-qPCR (n=4). **H)** Flow cytometry analysis of IL17RB protein expression over time (n=4). Mean fluorescence intensity (ΔMFI) was calculated as the difference between IL17RB MFI and isotype control MFI. Data are presented as mean ± SEM. RT-qPCR was normalized to 18SrRNA expression levels. *p<0.05, **p<0.01, ***p<0.001, ****p<0.0001. Schematic illustrations were Created in BioRender. Silva, L. (2027) https://BioRender.com/5t8bf7g.

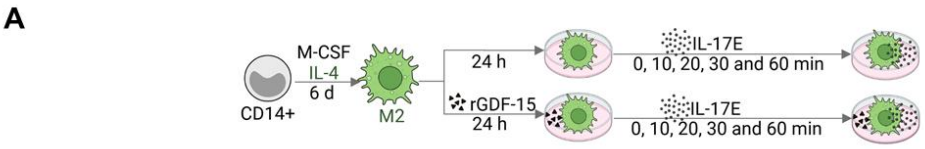
In the transcriptomic analysis, IL17RB was significantly upregulated in M0 and M2 cells under rGDF-15 treatment (fold changes of 2.02 and 1.66, respectively). However, expressions of IL-17E (ligand) and IL-8 (downstream cytokine) were unchanged, indicating that rGDF-15 treatment did not influence their expression. We validated IL17RB expression RNA seq data by RT-qPCR across all macrophage phenotypes, showing the highest expression in M2 (Fig. 3C). We additionally included an inflammatory challenge using LPS, as depicted in the diagram (Fig. 3A). After LPS challenge, M2 macrophages treated with rGDF-15 maintained significantly elevated

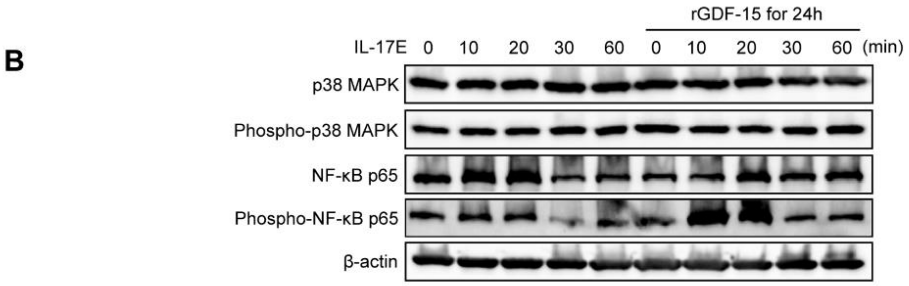
IL17RB expression compared with controls (Fig. 3D). We next evaluated IL17RB protein expression by flow cytometry, extending LPS exposure to 24 h. rGDF-15 significantly increased IL17RB protein levels in M2 macrophages, with a similar but non-significant trend after LPS challenge (Fig. 3E). Finally, to assess the persistence of the effect of rGDF-15 on IL17RB expression, M2 were incubated with rGDF-15 for a series of incubation times, including 24, 48, 72, and 96 h (Fig. 3F). IL17RB mRNA remained elevated up to 72 h but declined by 96 h (Fig. 3G). However, when the protein expression was assessed by flow cytometry, an increased IL17RB expression was also detected at this last time point (Fig. 3H), indicating a sustained impact of rGDF-15 on IL17RB expression in human macrophages.

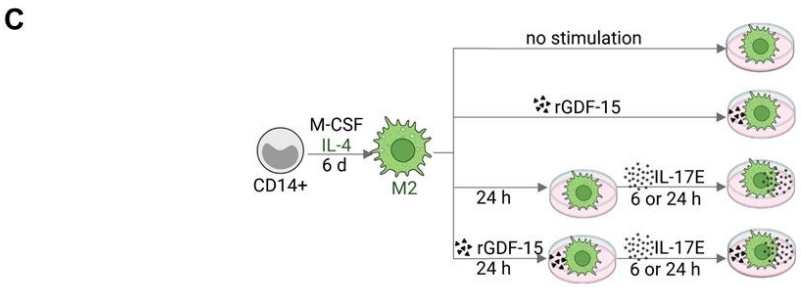
rGDF-15 modulates IL-17E/IL17RB signaling and reduces pro-inflammatory cytokine production

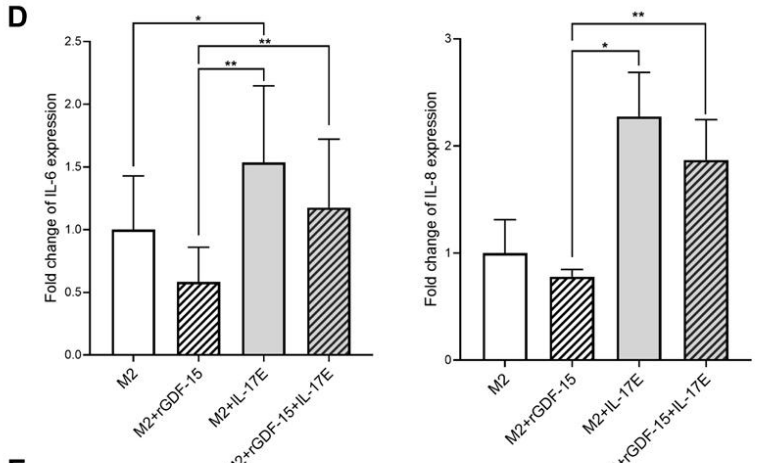
We analyzed whether IL17RB, induced by rGDF-15 in human macrophages, is functional and can drive signal transduction. M2 macrophages were exposed to rGDF-15 for 24 h, and then stimulated by IL-17E, ligand of IL17RB, for 10 to 60 min (Fig. 4A). We analyzed the phosphorylation state of two major IL17RB activation pathways, p38 MAPK and NF-κB p65, by Western blotting. rGDF-15 pretreatment enhanced NF-κB p65 phosphorylation within 10 min of IL-17E stimulation, peaking at 10-20 min and remaining elevated compared to the non-stimulated controls for up to 60 min. In contrast, p38 MAPK phosphorylation was not stimulated by IL17E (Fig. 4B). The next question was how rGDF-15 affects the outcome of IL-17E/IL17RB activation in terms of the production of two pro-inflammatory cytokines, IL-6 and IL-8, which have known pro-tumoral activity (Fig.4C). As expected, IL-17E in the absence of rGDF-15 increased IL-6 and IL-8 expression in M2 macrophages (Fig. 4D, 4E). rGDF-15 alone had no significant effect on the cytokine expression. However, rGDF-15 pretreatment

489 significantly attenuated IL-6 and IL-8 induction by IL-17E, particularly IL-8 production
490 at 24 h (Fig. 4E, F). Although rGDF-15 pretreatment increased NF-κB pathway
491 activation, the overall downstream output indicates that rGDF-15 exerts an inhibitory
492 effect on inflammatory cytokine production independently of the activated signal
493 transduction.


A
M-CSF
IL-4
6 d
CD14+
M2
24 h
rGDF-15
24 h
IL-17E
0, 10, 20, 30 and 60 min
IL-17E
0, 10, 20, 30 and 60 min


B
rGDF-15 for 24h
IL-17E 0 10 20 30 60 0 10 20 30 60 (min)
p38 MAPK
Phospho-p38 MAPK
NF-κB p65
Phospho-NF-κB p65
β-actin


C
no stimulation
rGDF-15
M-CSF
IL-4
6 d
CD14+
M2
24 h
IL-17E
6 or 24 h
rGDF-15
24 h
IL-17E
6 or 24 h


D
Fold change of IL-6 expression
Fold change of IL-8 expression
M2
M2+rGDF-15
M2+IL-17E
M2+rGDF-15+IL-17E

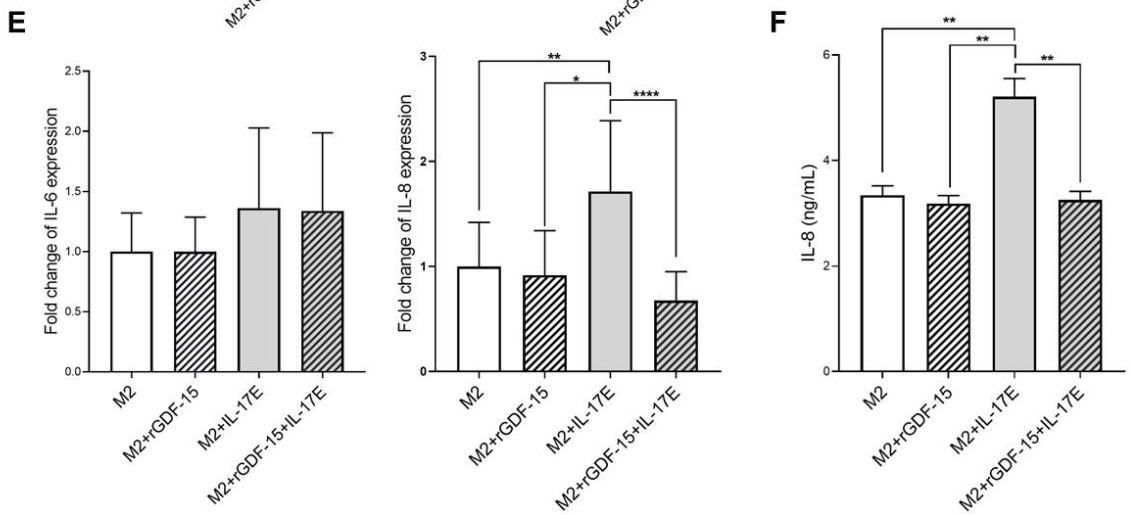

E
F
Fold change of IL-6 expression
Fold change of IL-8 expression
IL-8 (ng/mL)
M2
M2+rGDF-15
M2+IL-17E
M2+rGDF-15+IL-17E

Fig. 4. rGDF-15 effects on IL-17E/IL-17RB-mediated NF-κB p65 and p38 MAPK phosphorylation and cytokine expression in macrophages. A) Experimental design to explore the effect of rGDF-15 on IL-17RB-activated signaling pathways. On day 6 of M2 differentiation, cells were incubated in absence or presence of rGDF-15 (50 ng/mL) for 24 h, then stimulated with IL-17E (100 ng/mL) for 0, 10, 20, 30, and 60 min. Cells were collected for protein extraction and subsequent Western blot analysis. **B)** Western blot analyses of p38 MAPK, phospho-p38 MAPK, NF-κB p65, phospho-NF-κB p65, and β-actin were performed. Representative donor is shown. **C)** Experimental design for cytokine expression analysis. On day 6 of M2 differentiation, cells were treated ± 50 ng/mL rGDF-15 for 24 h, then stimulated with IL-17E (100 ng/mL) for 6 h or 24 h. **D)** RT-qPCR analysis of IL-6 and IL-8 gene expression in M2 macrophages after 6 h IL-17E stimulation (n=4). **E)** RT-qPCR analysis of IL-6 and IL-8 gene expression in M2 macrophages after 24 h IL-17E stimulation (n=6). **F)** IL-8 secretion analysis by ELISA in M2 macrophages after 24 h IL-17E stimulation (n=8). Data are presented as mean ± SEM. RT-qPCR was normalized to 18SrRNA expression levels. *$p < 0.05$, **$p < 0.01$, ***$p < 0.001$, and ****$p < 0.0001$. Schematic illustrations were Created in BioRender. Silva, L. (2027) https://BioRender.com/5t8bf7g.

We investigated the mechanisms underlying the anti-inflammatory effects of rGDF-15. Confocal microscopy showed that rGDF-15 did not inhibit NF-κB nuclear translocation (Supplementary Fig. 1), prompting us to examine alternative regulatory signaling pathways (Fig. 5A). First, we examined STAT6 activation, a key signaling pathway responsible for the anti-inflammatory macrophage programming. We analyzed monocyte-derived macrophages from nine independent donors and found that in eight of nine macrophage cultures, STAT6 phosphorylation was clearly increased between 30 and 120 min after rGDF-15 stimulation (Fig. 5B). To assess the involvement of TGF-β type I receptor (TGFBR1, also known as ALK5), macrophages were pretreated with HY-12043 (SB-525334), a potent and highly selective inhibitor of TGFBR1, for 1 h

before stimulation with rGDF-15. Application of HY-12043 suppressed GDF-15-induced enhancement of STAT6 phosphorylation (Fig. 5B). We next examined whether GDF-15 can induce Smad2/3 phosphorylation and found a positive effect in four analyzed monocyte-derived macrophage cultures; the effect was also abrogated by the pretreatment with HY-12043 (Fig. 5C).

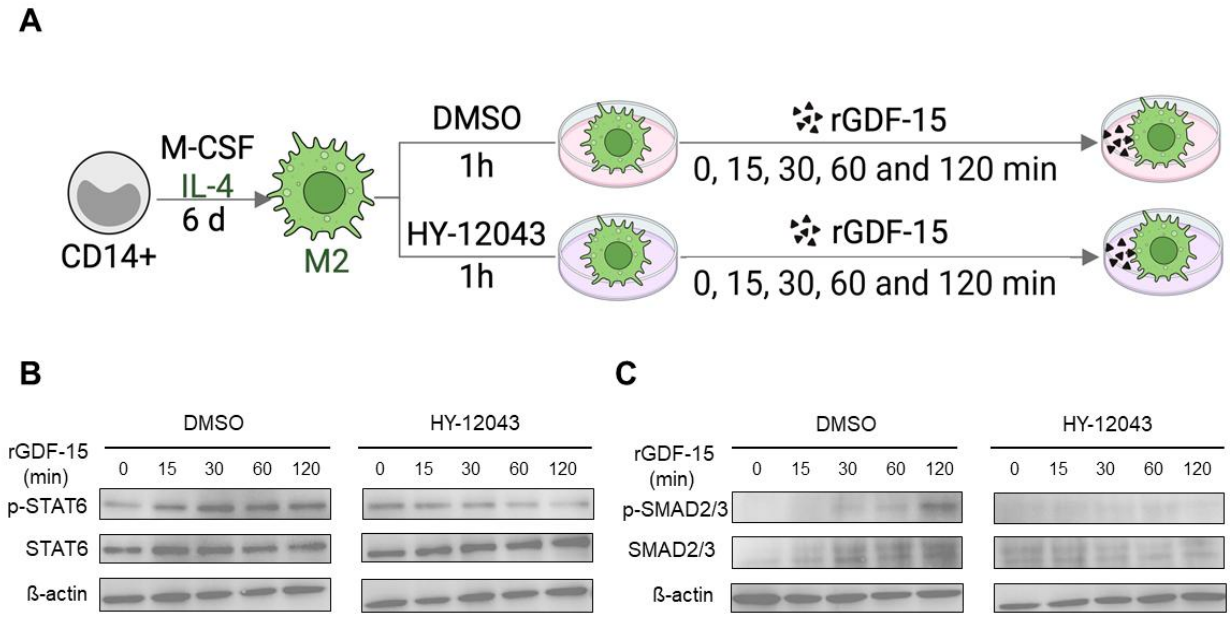


Fig. 5. GDF-15 activates anti-inflammatory pathways in primary human macrophages in a TFBR1-dependent way. A) Experimental design to explore downstream anti-inflammatory pathways activated by rGDF-15. On day 6 of M2 differentiation, cells were preincubated for 1 h with the highly selective inhibitor of TGFBR1, HY-12043 (SB-525334) at 1 µM and then treated with rGDF-15 (50 ng/mL) for 0, 15, 30, 60 and 120 min. Cells were collected for protein extraction and subsequent Western blot analysis. **B)** Western blot analysis of STAT6, phospho-STAT6 and β-actin were performed (n=9). Representative donor is shown. **C)** Western blot analysis of SMAD2/3, phospho-SMAD2/3 and β-actin were performed. Representative donor is shown (n=4). Schematic illustrations were Created in BioRender. Silva, L. (2027) https://BioRender.com/5t8bf7g.

Targeted analysis of the RNA seq dataset showed that rGDF-15 did not significantly induce the canonical NF-κB negative regulators NFKBIA, TNFAIP3, SOCS1, or SOCS3. In contrast, the inhibitory SMADs SMAD6 and SMAD7 were upregulated, indicating induction of a regulatory transcriptional program rather than classical NF-κB negative feedback (Supplementary Table 1).

We concluded that GDF-15 can amplify at least two anti-inflammatory signaling pathways in macrophages: STAT6 and Smad2/3, resulting in the IL-17E-induced NF-κB signaling outcome. TGFBR1 was required for the rGDF-15-mediated stimulation of both STAT6 and Smad2/3 signaling.

GDF-15 expression and clinical implications in clear cell renal cell carcinoma

Given that several key cancer-related pathways were upregulated in our transcriptomic analysis, we examined GDF-15 mRNA levels across various tumor types based on TCGA data. GDF-15 was significantly overexpressed in breast, colon, lung, prostate, and gastric tumors compared with healthy tissues, but was reduced in tumor tissue from patients with ccRCC. No significant difference was observed in bladder cancer (Fig. 6A). Next, we examined this finding in normal adjacent renal tissue versus ccRCC tissue and found similar results regarding GDF-15 expression. GDF-15 expression was higher in normal tissue than in ccRCC tissue (Fig. 6B). IL-17RB expression levels were likewise elevated in normal adjacent renal tissue compared to ccRCC tissue. However, IL-8 expression levels did not differ between the two tissues. Survival analysis of TCGA expression data showed that higher IL17RB expression in tumor tissue was associated with better OS and DSS. In contrast, high IL-8 expression levels were indicative of poor survival outcomes (Fig. 6C). No significant survival association was observed for tumor GDF15 expression. This may, in part, reflect the contribution of GDF-15 produced outside the tumor tissue, which is not captured by tumor transcriptomic data. Given

that GDF-15 reduced IL-8 production in IL-17E-stimulated macrophages and that IL-8 can modulate $CD8^+$ T-cell responses in cancer, we next explored whether tumor GDF15 expression was associated with estimated $CD8^+$ T-cell infiltration. In tumor-purity-adjusted TIMER analyses, GDF15 expression negatively correlated with estimated $CD8^+$ T-cell infiltration (partial Spearman's $\rho = -0.284$, $p < 0.00001$) (Supplementary Figure 2).

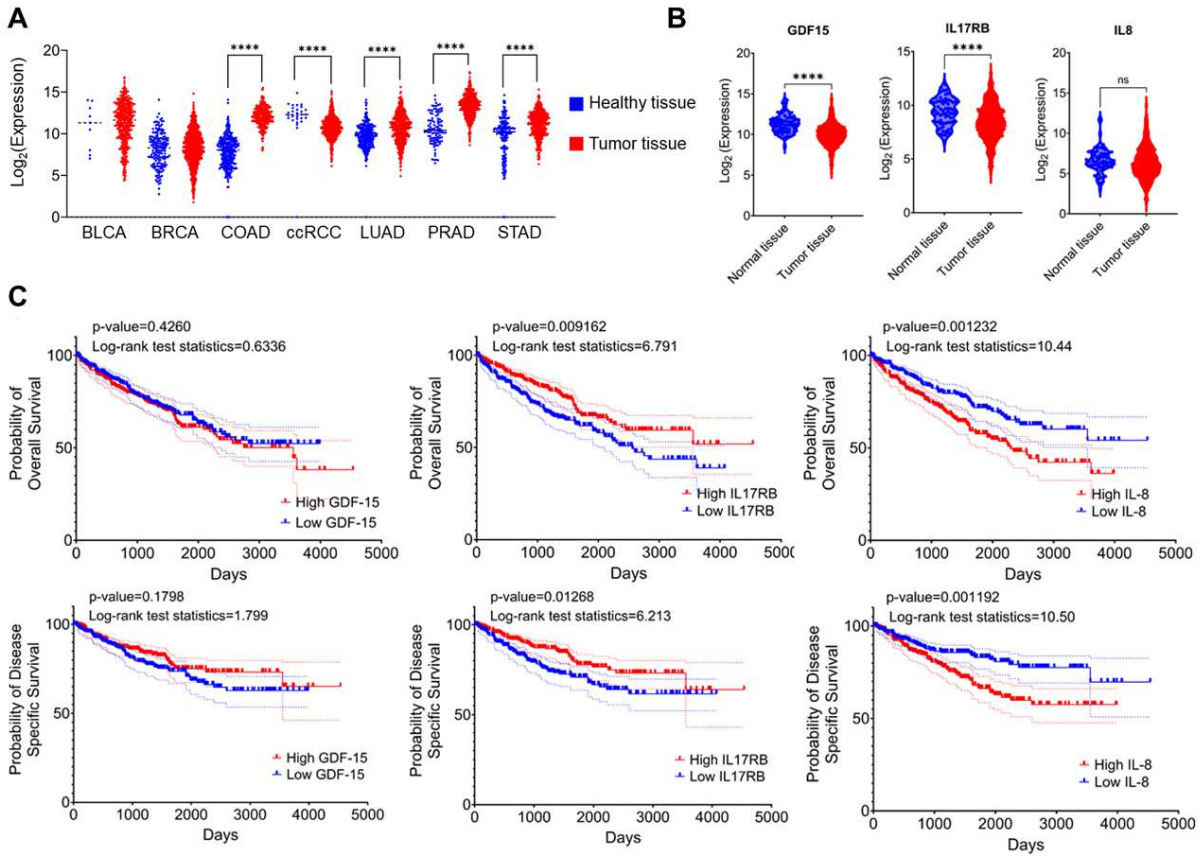


Fig. 6. Expression of GDF-15, IL17RB, and IL-8 and prognostic significance in ccRCC from the TCGA cohort. A) GDF-15 mRNA expression levels across different tumor types compared with normal tissue expression using the TCGA database. **B)** GDF-15, IL17RB and IL-8 mRNA expression level in ccRCC and their paired normal tissues. **C)** Kaplan-Meier curves for tissue-specific GDF-15, IL17RB, and IL-8 expression levels on overall survival and disease-specific survival of ccRCC patients. BLCA: Bladder Urothelial Carcinoma (n=9;407), BRCA: Breast Invasive Carcinoma (n=179;1092), COAD: Colon Adenocarcinoma (n=308;288), ccRCC: clear cell renal cell carcinoma (n=28;530), LUAD: Lung Adenocarcinoma (n=288;513),

PRAD: Prostate Adenocarcinoma (n=100;495), STAD: Stomach Adenocarcinoma (n=174;414). Data are presented as mean ± SEM. ****p<0.0001.

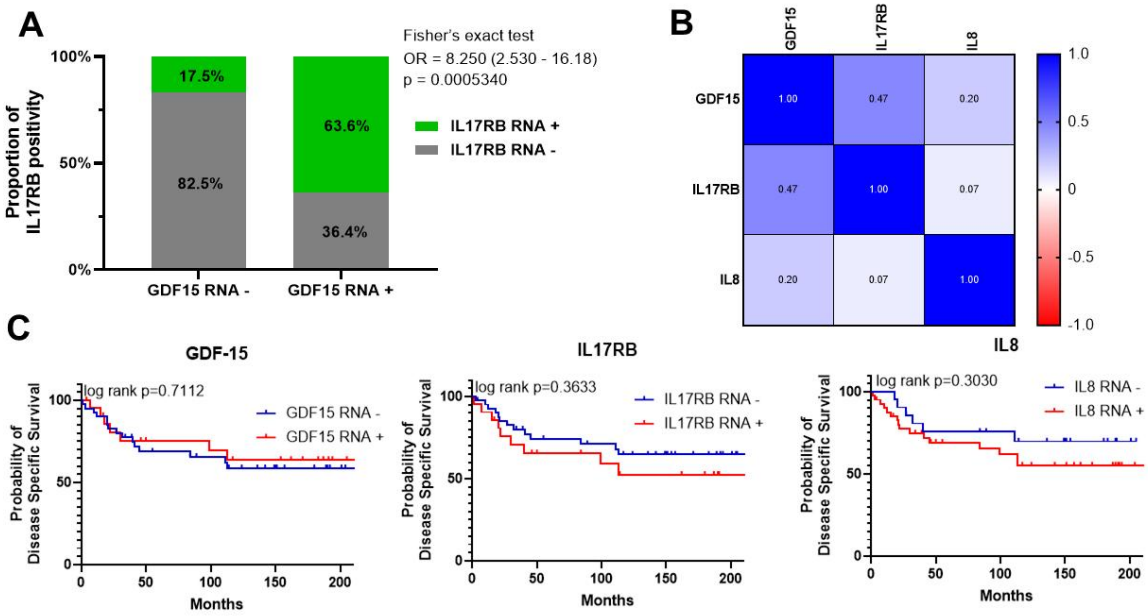
We next evaluated GDF15, IL17RB, and IL8 expression in tumor tissue from the ccRCC patient cohort from the Mannheim Medical Faculty, Heidelberg University (n=62 patients; 40.33% women, 59.67% men, mean age 63.7 years) (Table 2). Thirty-two patients had T1-T2 tumors, and 88% had a grade of G1-G2. GDF15 and IL17RB expression was detectable in 35.48% and 33.87% of tumors, respectively. Detectable GDF15 expression was significantly associated with detectable IL17RB expression (Fisher's exact test, p = 0.0005; OR = 8.25, 95% CI 2.53–16.18) (Fig. 7A), whereas associations between GDF15 and IL8 expression levels (p = 0.0911) or between IL17RB and IL8 expression (p = 0.2697) did not reach statistical significance. Analysis of continuous expression levels similarly demonstrated a moderate positive correlation between GDF15 and IL17RB expression (Spearman's ρ = 0.474, p = 0.00013). In contrast, IL8 expression was not significantly correlated with either GDF15 or IL17RB expression (GDF15–IL8: Spearman's ρ = 0.20, p = 0.124; IL17RB–IL8: Spearman's ρ = 0.07, p = 0.589) (Fig. 7B).

Table 2. Baseline characteristics of study participants

	Women	**Men**	**Total**
n (%)	25 (40.33%)	37 (59.67%)	62
Age	65.36 ± 9.394	62.94 ± 12.06	63.65 ± 11.07
T stage			
T1- T2	14 (56%)	18 (48.65%)	32 (51.61%)
T3-T4	11 (44%)	19 (51.35%)	30 (48.39%)
Grading			

G1-G2	24 (96%)	32 (86.49%)	56 (88.71%)
G3-G4	1 (4%)	5 (13.51%)	6 (9.68%)
Metastasis after surgery			
Yes	7 (28%)	8 (21.62%)	15 (24.19%)
No	18 (72%)	29 (78.38%)	47 (75.81%)
Disease-free survival (months)	44.67 ± 36.54	37.15 ± 34.90	39.83 ± 35.24
GDF15 expression			
Yes	10 (40%)	12 (32.43%)	22 (35.48%)
No	15 (60%)	25 (67.57%)	40 (64.51%)
IL17RB expression			
Yes	7 (28%)	14 (37.84%)	21 (33.87%)
No	18 (72%)	23 (62.16%)	41 (66.13%)
IL8 expression			
Yes	17 (68%)	24 (64.86%)	41 (66.13%)
No	8 (32%)	13 (35.14%)	21 (33.87%)

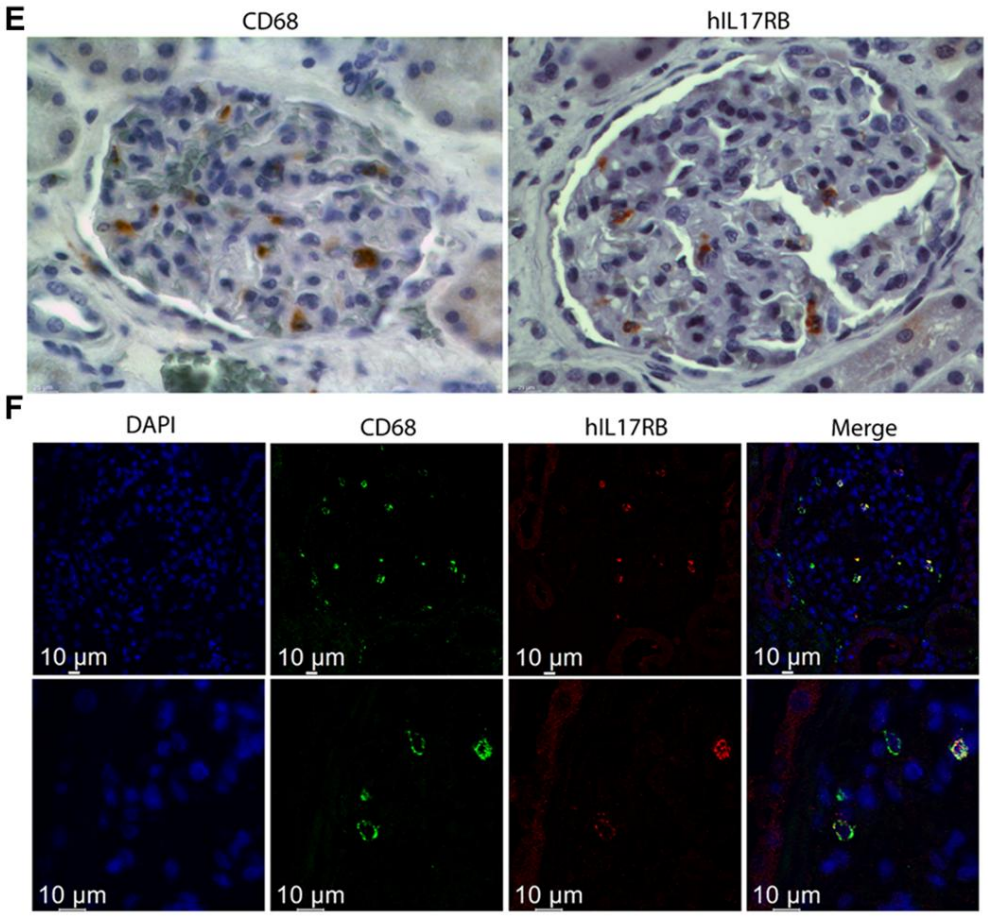
598 Data are means ±SD unless indicated otherwise.



D

Multivariable Cox regression analysis

Endpoint	Gene	HR (95% CI)	p
DSS	GDF15	0.74 (0.31–1.73)	0.516
	IL17RB	1.92 (0.78–4.72)	0.158
	IL8	2.84 (1.42–5.69)	**0.003**



599

Fig. 7. Expression and prognostic relevance of GDF15, IL17RB, and IL8 in the internal ccRCC cohort. A) Contingency analysis showing the association between GDF15 and IL17RB expression in tumor samples (n = 62). Gene expression was classified as detectable or non-detectable based on RT-qPCR measurements. Statistical significance was assessed using Fisher's exact test. **B)** Heatmap displaying Spearman correlation analysis values between gene expression levels of GDF-15, IL17RB and IL-8 from our internal ccRCC cohort. **C)** Kaplan-Meier curves showing disease-specific survival (DSS) according to tumor GDF15, IL17RB, and IL8 expression. For each gene, patients were stratified according to detectable versus non-detectable expression in tumor tissue. Differences between groups were assessed using the log-rank test. **D)** Multivariable Cox regression analysis of gene expression and survival outcomes in the ccRCC cohort. Multivariable Cox proportional hazards models were used to evaluate the associations of IL8, GDF15, and IL17RB expression with DSS. Separate models were fitted for each gene and adjusted for age at surgery, tumor stage, and metastatic status. Hazard ratios (HRs), 95% confidence intervals (CIs), and corresponding p values are shown. **E)** Representative immunohistochemical staining for CD68 (macrophage marker) and IL17RB in ccRCC tumor tissues from the internal cohort. **F)** Representative confocal immunofluorescence staining showing CD68 and IL17RB localization in ccRCC tumor sections from the same cohort. Nuclei were visualized using DAPI (blue). CD68 was detected using mouse monoclonal anti-human antibody and AlexaFluor488-conjugated donkey secondary antibody (visualized in green). IL17RB was detected by rabbit polyclonal anti-human antibody and Cy3-conjugated donkey secondary antibody (visualized in red). Colocalization of IL17RB and CD68 is visualized in yellow. Scale bars: 10 µm.

To assess whether the correlation between GDF15 and IL17RB was independent of clinicopathological characteristics, we fitted a multivariable logistic regression model including age at surgery, tumor stage, tumor grade, and metastatic status after surgery. GDF15 expression remained independently associated with IL17RB expression after adjustment for these variables (OR = 10.98, 95% CI 2.83–42.56, p = 0.0005)

(Supplementary Table 2), indicating that differences in disease stage, grade, metastatic status, or age did not explain the observed relationship.

Survival analyses were considered exploratory because of the limited cohort size and the predominance of localized, low-grade tumors. Kaplan-Meier analysis showed a non-significant tendency toward reduced DSS in patients with IL8-positive tumors compared with those with IL8-negative tumors (log-rank p = 0.30) (Fig. 6C). Neither GDF-15 nor IL17RB expression was associated with DSS in the unadjusted analyses (log-rank p = 0.71 and p = 0.36, respectively). In exploratory multivariable Cox models adjusted for age, tumor stage, and metastatic status, IL8 expression was associated with worse DSS (HR = 2.84, 95% CI 1.42–5.69), whereas GDF-15 (HR = 0.74, 95% CI 0.29–1.86) and IL17RB expression (HR = 1.92, 95% CI 0.78–4.75) were not (Fig. 7D).

Finally, we assessed whether IL17RB is expressed on the $CD68^{+}$ tumor-associated macrophages in ccRCC tissue by immunohistochemistry and confocal microscopy (Fig. 7E, F). IL17RB expression was observed almost exclusively in macrophages, highlighting macrophages as the primary cell type expressing IL17RB in response to GDF-15 stimulation of the ccRCC tumor microenvironment. To determine whether bulk-tumor IL17RB expression merely reflected macrophage abundance, we quantified CD68 expression by RT-qPCR in the internal cohort. CD68 and IL17RB expression were not significantly correlated (Spearman's $\rho = 0.21$, $p = 0.15$) (Supplementary Figure 3). Together with the in vitro induction of IL17RB by GDF-15, these findings argue towards IL17RB being not as a passive marker of macrophage infiltration, but rather as an indicator of GDF-15-induced transcriptome in TAMs in ccRCC.

Discussion

Currently, the immunosuppressive abilities of GDF-15 are considered a universal tumor-supportive mechanism in solid tumors. Targeting GDF-15 is believed to be an efficient way to reprogram immune-metabolic suppression and enhance the efficacy of checkpoint blockade. Recent clinical trials have provided very promising results for the application of GDF-15 blocking antibody in combination with anti-PD-1/PD-L1 immunotherapy in non-squamous non-small cell lung cancer and urothelial cancer (GDFATHER-01/2a trial) and muscle-invasive bladder cancer (GDFATHER-NEO trial) [14, 17]; and further stimulated interest in including more solid cancer types in clinical trials with neutralizing GDF-15 antibody. However, the mechanisms of intertumoral immunity and the specific contributions of immune cells differ across tumor localizations.

Our study provides the first comprehensive transcriptomic analysis of human macrophages exposed to GDF-15. Our findings expand the understanding of GDF-15 as an immunoregulatory cytokine, as we showed that GDF-15 induces a pro-angiogenic program and affects the cytokine and receptor expression profile in macrophages, such as IL17RB. At the same time, we showed that macrophages exposed to rGDF-15, in which the IL-17E/IL-17RB pathway was activated, were prevented from producing pro-inflammatory cytokines despite NF-κB activation. Mechanistically, for the first time, we identified the anti-inflammatory action of rGDF-15 in macrophages, acting through at least two mechanisms: enhancement of STAT6 phosphorylation and induction of Smad2/3 phosphorylation. Pharmacological inhibition of TGFBR1/ALK5 abrogated both signaling responses, supporting the involvement of TGFBR1-dependent signaling in GDF-15-induced macrophage programming.

First, we assessed the effect of rGDF-15 on TNF-α expression following LPS exposure. In all models tested, rGDF-15 reduced TNF-α expression after LPS challenge. This anti-inflammatory effect of GDF-15 has been well known since its discovery, but we extend these observations by demonstrating that this effect is evident at lower rGDF-15 doses (10 and 25 ng/mL) and LPS concentrations (100 ng/mL) than previously reported [30]. These findings highlight that macrophages are highly sensitive to GDF-15 modulation and are consistent with those of Dai et al., who recently identified a set of naturally occurring human monocyte-derived macrophages expressing high levels of GDF-15, that exhibited blunted inflammatory responses when challenged with LPS [42]. Possible pathways responsible for this phenotype shift have been proposed. For instance, some research groups proposed the decrease in phosphorylation of JAK1/STAT3, MAPK, and nuclear translocation of NF-κB after rGDF-15 treatment, or the activation of PI3K/AKT signaling pathway as potential mechanisms [43-45]. However, the specific pathway mediating GDF-15's anti-inflammatory effects in macrophages has not been thoroughly dissected.

Our transcriptomic results demonstrated that rGDF-15 induces specific transcriptional responses in activated macrophages, upregulating genes involved in angiogenesis, tissue remodeling, and innate immune activation. Together with the reduced inflammatory cytokine output observed in our functional experiments, these findings indicate that GDF-15 induces a multifaceted macrophage program. Macrophage activation encompasses a continuum of context-dependent states that cannot be adequately captured by a strict pro- versus anti-tumoral dichotomy [46]. TAMs may display overlapping angiogenic, migratory, tissue-remodeling, and immunoregulatory programs, whose functional consequences depend on tumor type, disease stage, spatial niche, and the surrounding cellular and cytokine environment [47-49]. The

transcriptomic data also revealed modulation of gene sets related to T-cell-associated immune processes. However, because these analyses were performed exclusively in macrophages, they do not demonstrate a direct effect of GDF-15 on T-cell function. Previous studies have shown that tumor-derived GDF-15 can inhibit LFA-1/ICAM-1-dependent T-cell recruitment and contribute to resistance to immune-checkpoint blockade, providing broader biological context for the immunoregulatory effects observed here [50]. In contrast, Zhou and colleagues showed that GDF15+ macrophages increase the overall recruitment and antigen-specific proliferation of CD8+ T-cells in a mouse oral squamous cell carcinoma model, compared with GDF15 negative macrophages emphasizing the context-dependent immunological effects of macrophage-derived GDF-15 may have distinct immunological effects [11]. Nevertheless, whether the macrophage program induced by GDF-15 indirectly influences T-cell recruitment, activation, exhaustion, or cytotoxicity in ccRCC remains to be determined using dedicated co-culture or in vivo models.

Among the most notable findings was the sustained upregulation of IL17RB, the receptor for IL-17E, in M0 and M2 macrophages. Increased surface IL17RB expression could potentiate IL-17E responsiveness, thereby amplifying signals for tissue repair and remodeling. Interestingly, although rGDF-15 pretreatment enhanced NF-κB p65 phosphorylation after IL-17E stimulation, it simultaneously reduced IL-6 and IL-8 gene expression, suggesting that GDF-15 biases IL-17E/IL17RB signaling toward a regulatory rather than proinflammatory outcome. This represents a novel mechanistic insight into how GDF-15 fine-tunes macrophage function and may reconcile its pro-angiogenic yet anti-inflammatory roles.

Although IL17RB is classically linked to tumor-promoting inflammation across several cancer types, we observed that its expression correlated with improved OS and DSS in ccRCC, as indicated by the TCGA cohort analysis [51-53]. This association was not reproduced in our smaller cohort, where IL17RB expression was not significantly associated with DSS in either the Kaplan-Meier or multivariable Cox analyses. Its prognostic relevance in ccRCC should therefore be considered exploratory and potentially dependent on cohort composition or tumor context. Nevertheless, IL17RB may identify a specific macrophage-associated transcriptional or activation state, as our histological analysis confirmed that IL17RB expression in ccRCC is almost exclusively restricted to CD68+ macrophages, underscoring their role as the principal cellular mediators of this pathway. Moreover, IL17RB expression did not correlate significantly with CD68 expression, indicating that its expression does not appear to reflect macrophage abundance alone.

Our results also have clinical relevance and potential therapeutic implications. IL-8 was associated with worse survival outcomes in ccRCC in the TCGA and in our cohort. This is consistent with published data from ccRCC cohorts, in which IL-8 in plasma, peripheral blood mononuclear cells, and the myeloid compartment in tumor tissue (as shown by single-cell RNA sequencing) were associated with decreased efficacy of atezolizumab immune checkpoint blockade [12]. At the genetic level, polymorphisms that provided higher expression of IL8 were linked to poorer survival in patients treated with the tyrosine kinase inhibitors pazopanib or sunitinib [54]. IL-8 is a potent driver of cytotoxic T cells, which, in the majority of tumors, provide strongly beneficial anti-tumor immune responses for the patient [55, 56]. Recently, it was shown for advanced colorectal cancer that IL-8 derived from macrophages can inhibit $CD8^+$ T-cell function by downregulating TIM3 [57]. T-cell biology in ccRCC appears to be complex. scRNA

seq analysis revealed several subclusters characterized by the expression of TYMP, TOP2A, CHI3L2, CDKN3, CENPM, and EZH2, correlating with poor prognosis. Among these sub-clusters, $CD8^+$ T-cells were identified as potentially playing a critical role in mediating ccRCC metastasis [58]. Another study showed that in patients with ccRCC, intratumoral $CXCL13^+CD8^+$T-cells infiltration indicated worse clinical outcome, was associated with immunoreactive contexture, and $CXCL13^+CD8^+$T-cells possessed an exhausted phenotype and decreased effector molecules. Analysis of combined RCC cohorts, encompassing more than 1,400 patients, demonstrated that high infiltration of lactate-programmed TAMs, producing IL-8, associates with $CD8^+$ T-cell exhaustion and immune checkpoint blockade resistance [59]. Thus, data accumulated about IL-8-mediated suppression of $CD8^+$ T-cell cytotoxicity, and our data on the rGDF-15 downregulated IL-8 expression in macrophages may reflect an important mechanism by which GDF-15 contributes to a less aggressive tumor phenotype [12]. Targeting IL-8 is under investigation in other solid tumors, and our findings suggest that such approaches could be explored in ccRCC, particularly in patients with low GDF-15 expression [60].

Our findings should also be considered alongside tumor cell-intrinsic mechanisms of GDF-15 in ccRCC. Previous work showed that GDF15 downregulation in ccRCC cells reduces lipid peroxidation and intracellular iron accumulation through increased GPX4 expression, thereby suppressing ferroptosis and promoting tumor-cell viability and aggressiveness [61]. In our macrophage RNA seq dataset, rGDF-15 did not induce a clear ferroptosis-related transcriptional signature, although transcriptomic analysis alone cannot exclude this mechanism. Thus, GDF-15 may exert compartment-specific effects in ccRCC through both tumor cell-intrinsic regulation and macrophage-directed immune modulation.

Recent findings provide further evidence for the context-dependent role of GDF-15 in ccRCC. Akdogan et al. reported that high tumor GDF-15 protein expression was associated with reduced anti-PD-1 response and shorter progression-free and OS in 46 patients with metastatic ccRCC [62]. These findings contrast with the tendency toward more favorable OS associated with GDF15 expression in our cohort. However, important differences between the study populations should be considered. Whereas Akdogan et al. exclusively investigated patients with metastatic disease receiving immune checkpoint inhibition, our cohort comprised patients with initially non-metastatic, predominantly low-grade tumors and no previous exposure to immunotherapy. Differences in disease stage and treatment context may contribute to divergent observations, suggesting that the biological and clinical significance of GDF-15 may depend on the tumor microenvironment and therapeutic setting. Supporting this possibility, Husaini et al. demonstrated in a prostate cancer mouse model that GDF-15 overexpression suppressed primary tumor growth while promoting metastatic dissemination at later stages [63]. Whether similar stage-dependent effects occur in ccRCC remains to be established.

Finally, our data raise important considerations for GDF-15-targeted therapies. Early-phase clinical trials of GDF-15 neutralization (e.g., visugromab combined with nivolumab) have shown encouraging responses in anti-PD-1-refractory cancers [14, 16, 17]. Although GDF-15 inhibition may enhance antitumor immunity by facilitating T-cell infiltration and improving responses to checkpoint blockade, our findings suggest that it can suppress macrophage-mediated pro-tumoral inflammatory responses in ccRCC. Nevertheless, the potential benefits or risks of GDF-15 inhibition in ccRCC must be considered in the context of disease stage and treatment. The potential risks

in ccRCC require careful patient selection and biomarker development before considering GDF-15-targeted therapies.

Our study provides new insights into the function of GDF-15 in the macrophage system. However, we must acknowledge limitations. First, macrophages were modeled using M0, M1, and M2 polarization states, which do not fully capture the heterogeneity of tumor-associated macrophages in vivo [64]. Thus, understanding macrophage activation and function in response to GDF-15 remains far from complete, and future studies should explore a broader range of activation states and their functions, including single-cell RNA sequencing and spatial transcriptomics. Second, the receptor(s) mediating GDF-15's effect on macrophages remain to be identified. Neither GFRAL nor RET was detectably expressed in our macrophage transcriptomic dataset, arguing against canonical GFRAL/RET signaling under the conditions examined. Pharmacological inhibition of TGFBR1 abrogated GDF-15-induced STAT6 and Smad2/3 phosphorylation, supporting the involvement of TGFBR1-dependent signaling. However, these findings do not establish TGFBR1 as a direct receptor for GDF-15, and genetic validation and ligand-receptor binding studies are required.
Our clinical cohort was relatively small, limiting the study's statistical power and the generalizability of the findings. As a result, subtle differences in gene expression may not have reached statistical significance, and observed associations should be interpreted with caution. Also, our data may not generalize to patients with advanced-stage or metastatic disease, where tumor-immune interactions and inflammatory signaling pathways may differ substantially, as our cohort comprised mostly localized, low-grade tumors. Because no healthy adjacent tissue was available in our cohort, we could not perform intra-patient comparisons or analyze inter-individual variability. To address this limitation, we assessed publicly available gene expression data sets,

which allowed us a broader understanding of the gene expression in ccRCC. Further studies with larger cohorts, including normal control tissues and functional validation, will be essential to confirm and extend the associations between GDF-15, IL17RB, IL-8, and patient outcomes. In vivo studies using mice ccRCC models are also required to determine whether GDF-15 supplementation or inhibition directly alters tumor growth, angiogenesis, or immunotherapy responsiveness. In addition, diverse sources of IL-17E that contribute to activating the IL-17RB pathway need to be explored. Whether tumor cells, healthy kidney cells or other stromal counterparts directly produce IL-17E remains an open question.

Conclusion

Our findings provide new insight into the role of GDF-15 in shaping macrophage function, identify new signaling and receptor mechanisms mediating GDF-15 anti-inflammatory effects, and provide evidence for the beneficial role of GDF-15 in the ccRCC tumor microenvironment. GDF-15 upregulates IL17RB expression, modulates IL-17E/IL17RB signaling, suppresses proinflammatory cytokine production, particularly IL-8, and utilizes anti-inflammatory STAT6 and Smad2/3 signaling pathways via TGFBR1. These data suggest that GDF-15 promotes a regulatory, tissue-remodeling macrophage program that may have context-dependent relevance in ccRCC. The favorable association of IL17RB with survival, together with its predominant localization in tumor-associated macrophages, supports further investigation of the GDF-15/IL17RB axis as a potentially clinically relevant macrophage-associated pathway. A deeper understanding of the GDF-15/IL17RB axis and its interaction with immunotherapies will be critical for guiding the use of GDF-15-targeted strategies in ccRCC.

List of abbreviations

anti-PD-1, anti-programmed cell death protein 1

anti-PD-L1, anti-programmed death-ligand 1

CAR, chimeric antigen receptor

ccRCC, clear cell renal cell carcinoma

CI, confidence interval

DC, dendritic cell

DSS, disease-specific survival

ELISA, enzyme-linked immunosorbent assay

FDR, false discovery rate

FPKM, fragments per kilobase of transcript per million mapped reads

GDF-15, growth differentiation factor 15

GDNF, glial cell line-derived neurotrophic factor

GEO, Gene Expression Omnibus

GFRAL, GDNF family receptor α-like

GO, Gene Ontology

HR, hazard ratio

HRP, horseradish peroxidase

IL17RB, interleukin-17 receptor β

LPS, lipopolysaccharide

MACS, magnetic-activated cell sorting

MAPK, mitogen-activated protein kinase

M-CSF, macrophage colony-stimulating factor

MFI, mean fluorescence intensity

MIC-1, macrophage inhibitory cytokine-1

NES, normalized enrichment score

NF-κB, nuclear factor κB

NFKBIA, NF-κB inhibitor α

OS, overall survival

RET, RET receptor tyrosine kinase

rGDF-15, recombinant human GDF-15

RNA-seq, RNA sequencing

SEM, standard error of the mean

SMAD2/3, SMAD proteins 2 and 3

SMAD6/7, inhibitory SMAD proteins 6 and 7

SOCS1/3, suppressor of cytokine signaling 1 and 3

STAT6, signal transducer and activator of transcription 6

TAM, tumor-associated macrophage

TCGA, The Cancer Genome Atlas

TGF-β, transforming growth factor β

TIMER, Tumor Immune Estimation Resource

TLR, Toll-like receptor

TNF-α, tumor necrosis factor α

TNFAIP3, tumor necrosis factor α-induced protein 3

Declarations

Ethics approval and consent to participate

The study was approved by the institutional ethics committee of the Medical Faculty of Mannheim from the Heidelberg University (ethics approval 2015-549N-MA and 2024-591-MA).

Consent for publication

No applicable

Availability of data and materials

The original RNA seq data for all differentially activated genes is available on the NCBI Gene Expression Omnibus (GEO) browser (Reference number GSE308883).

Competing interests

The authors declare that they have no competing interests

Funding

This work was supported by an internal grant of the German Red Cross Blood Donor Service Baden-Wuerttemberg-Hessen, Germany. For the publication fee, we acknowledge financial support from Heidelberg University.

Authors' contributions

LSSB: Conceptualization, Methodology, Investigation, Software, Formal Analysis, Writing- Original draft. **JX**: Conceptualization, Methodology, Validation, Investigation, Formal analysis. **NAA:** Methodology, Investigation. **JZ:** Methodology, Investigation.

CS: Validation, Investigation. **AKN:** Methodology, Investigation. **KN:** Resources, Writing – Review & Editing. **TW:** Resources, Writing – Review & Editing. **BR:** Resources, Writing – Review & Editing. **CB:** Resources, Writing – Review & Editing. **CW:** Formal Analysis, Writing – Review & Editing. **HK:** Resources, Writing – Review & Editing. **JK:** Supervision, Conceptualization, Writing - Original Draft, Investigation, Formal analysis, Funding acquisition, Project administration.

Acknowledgements

We thank the Live Cell Imaging Mannheim (LIMa) Core Facility of the Medical Faculty Mannheim at Heidelberg University for their assistance with immunofluorescence staining and confocal microscopy. Likewise, we would like to acknowledge Stefanie Uhlig from the FlowCore at the same institution for technical and consultative support in flow cytometry.

References

1. Tsai VWW, Husaini Y, Sainsbury A, Brown DA, Breit SN. The MIC-1/GDF15-GFRAL Pathway in Energy Homeostasis: Implications for Obesity, Cachexia, and Other Associated Diseases. Cell Metab. 2018;28(3):353–68. doi: 10.1016/j.cmet.2018.07.018
2. Silva-Bermudez LS, Kluter H, Kzhyshkowska JG. Macrophages as a Source and Target of GDF-15. Int J Mol Sci. 2024;25(13). doi: 10.3390/ijms25137313
3. Emmerson PJ, Wang F, Du Y, Liu Q, Pickard RT, Gonciarz MD, et al. The metabolic effects of GDF15 are mediated by the orphan receptor GFRAL. Nat Med. 2017;23(10):1215–9. doi: 10.1038/nm.4393
4. Mullican SE, Lin-Schmidt X, Chin CN, Chavez JA, Furman JL, Armstrong AA, et al. GFRAL is the receptor for GDF15 and the ligand promotes weight loss in mice and nonhuman primates. Nat Med. 2017;23(10):1150–7. doi: 10.1038/nm.4392
5. Hullwegen M, Kleinert M, von Haehling S, Fischer A. GDF15: from biomarker to target in cancer cachexia. Trends Cancer. 2025. doi: 10.1016/j.trecan.2025.06.007
6. Wang Z, Wang S, Jia Z, Hu Y, Cao D, Yang M, et al. YKL-40 derived from infiltrating macrophages cooperates with GDF15 to establish an immune suppressive microenvironment in gallbladder cancer. Cancer Lett. 2023;563:216184. doi: 10.1016/j.canlet.2023.216184
7. Zheng H, Yu S, Zhu C, Guo T, Liu F, Xu Y. HIF1alpha promotes tumor chemoresistance via recruiting GDF15-producing TAMs in colorectal cancer. Exp Cell Res. 2021;398(2):112394. doi: 10.1016/j.yexcr.2020.112394
8. Yu S, Li Q, Yu Y, Cui Y, Li W, Liu T, et al. Activated HIF1alpha of tumor cells promotes chemoresistance development via recruiting GDF15-producing tumor-associated

965 macrophages in gastric cancer. Cancer Immunol Immunother. 2020;69(10):1973–87. doi:
966 10.1007/s00262-020-02598-5
967 9. Zhu W, Xu H, Xiong X, Li Y, Feng D, Huang W, et al. Decoding GDF15: Impact on
968 prostate cancer metabolism, chemoresistance, and clinical applications. Chin Med J (Engl).
969 2025. doi: 10.1097/CM9.0000000000003876
970 10. Lu L, Johnson CH, Khan SA, Irwin ML. GDF15 in the tumor microenvironment: A central
971 mediator of cancer immunometabolism and therapeutic resistance. Cytokine Growth Factor
972 Rev. 2026;88:47–57. doi: 10.1016/j.cytogfr.2026.01.004
973 11. Zhou X, Zhou Z, Ju H, Guo C, Zhu F, Zhang Y, et al. Context-Dependent Role of
974 GDF15: GDF15(+) Tumor-Associated Macrophages Suppress OSCC Progression by
975 Enhancing Phagocytosis. Adv Sci (Weinh). 2026;13(29):e18525. doi:
976 10.1002/advs.202518525
977 12. Dai S, Zeng H, Liu Z, Jin K, Jiang W, Wang Z, et al. Intratumoral CXCL13(+)CD8(+)T
978 cell infiltration determines poor clinical outcomes and immunoevasive contexture in patients
979 with clear cell renal cell carcinoma. J Immunother Cancer. 2021;9(2). doi: 10.1136/jitc-2020-
980 001823
981 13. Sigvardsen CM, Richter MM, Engelbeen S, Kleinert M, Richter EA. GDF15 is still a
982 mystery hormone. Trends Endocrinol Metab. 2025;36(6):591–601. doi:
983 10.1016/j.tem.2024.09.002
984 14. Melero I, de Miguel Luken M, de Velasco G, Garralda E, Martin-Liberal J, Joerger M,
985 et al. Neutralizing GDF-15 can overcome anti-PD-1 and anti-PD-L1 resistance in solid tumours.
986 Nature. 2025;637(8048):1218–27. doi: 10.1038/s41586-024-08305-z
987 15. Sugiyama K, Starling N, Chau I. New Horizons with Growth Differentiation Factor 15 in
988 Oncology: From Cancer Cachexia and Tumour Immunity to Novel Therapeutic Strategies. Curr
989 Oncol. 2025;32(11). doi: 10.3390/curroncol32110604
990 16. Melero I, de Miguel M, Cabanas EG, de Velasco G, Joerger M, Martin-Liberal J, et al.
991 Long-term follow-up of a phase 1/2 trial of anti-GDF-15 antibody visugromab plus anti-PD-1
992 antibody nivolumab in anti-PD-1/-L1 relapsed/refractory solid tumors. J Hematol Oncol.
993 2026;19(1). doi: 10.1186/s13045-026-01818-2
994 17. Necchi A, Mercinelli C, Maiorano BA, Piacentini M, Cigliola A, Iacovelli R, et al.
995 Neoadjuvant nivolumab with or without visugromab in muscle-invasive bladder cancer: the
996 phase 2a GDFATHER-NEO trial. Nat Med. 2026. doi: 10.1038/s41591-026-04740-9
997 18. Kzhyshkowska J, Shen J, Larionova I. Targeting of TAMs: can we be more clever than
998 cancer cells? Cell Mol Immunol. 2024;21(12):1376–409. doi: 10.1038/s41423-024-01232-z
999 19. Larionova I, Kazakova E, Gerashchenko T, Kzhyshkowska J. New Angiogenic
1000 Regulators Produced by TAMs: Perspective for Targeting Tumor Angiogenesis. Cancers
1001 (Basel). 2021;13(13). doi: 10.3390/cancers13133253
1002 20. Kazakova E, Iamshchikov P, Larionova I, Kzhyshkowska J. Macrophage scavenger
1003 receptors: Tumor support and tumor inhibition. Front Oncol. 2022;12:1096897. doi:
1004 10.3389/fonc.2022.1096897
1005 21. Larionova I, Kazakova E, Patysheva M, Kzhyshkowska J. Transcriptional, Epigenetic
1006 and Metabolic Programming of Tumor-Associated Macrophages. Cancers (Basel). 2020;12(6).
1007 doi: 10.3390/cancers12061411
1008 22. Bleriot C, Dunsmore G, Alonso-Curbelo D, Ginhoux F. A temporal perspective for
1009 tumor-associated macrophage identities and functions. Cancer Cell. 2024;42(5):747–58. doi:
1010 10.1016/j.ccell.2024.04.002
1011 23. Wang X, He J, Ding G, Tang Y, Wang Q. Overcoming resistance to PD-1 and CTLA-4
1012 blockade mechanisms and therapeutic strategies. Front Immunol. 2025;16:1688699. doi:
1013 10.3389/fimmu.2025.1688699
1014 24. Varmazyari S, Borhani H, Moradipour Z, Ziaei H, Rezaei N. Characterizing the Head
1015 and Neck Cancer Microenvironment: Implications for Immunotherapy and Prognosis. Adv Exp
1016 Med Biol. 2026;1492:363–97. doi: 10.1007/978-3-032-03176-1_18
1017 25. Takenouchi Y, Kitakaze K, Tsuboi K, Okamoto Y. Growth differentiation factor 15
1018 facilitates lung fibrosis by activating macrophages and fibroblasts. Exp Cell Res.
1019 2020;391(2):112010. doi: 10.1016/j.yexcr.2020.112010

26. Miyake M, Zhang J, Yasue A, Hisanaga S, Tsugawa K, Sakaue H, et al. Integrated stress response regulates GDF15 secretion from adipocytes, preferentially suppresses appetite for a high-fat diet and improves obesity. iScience. 2021;24(12):103448. doi: 10.1016/j.isci.2021.103448
27. Urakawa N, Utsunomiya S, Nishio M, Shigeoka M, Takase N, Arai N, et al. GDF15 derived from both tumor-associated macrophages and esophageal squamous cell carcinomas contributes to tumor progression via Akt and Erk pathways. Lab Invest. 2015;95(5):491–503. doi: 10.1038/labinvest.2015.36
28. Lu QW, Liao Y. GDF-15 upregulates the SLC7A11/GPX4 signaling axis and promotes mitoxantrone resistance in AML cells. Eur J Med Res. 2025;30(1):504. doi: 10.1186/s40001-025-02787-x
29. Zhang X, Dong S. Protective effect of growth differentiation factor 15 in sepsis by regulating macrophage polarization and its mechanism. Bioengineered. 2022;13(4):9687–707. doi: 10.1080/21655979.2022.2059903
30. Li H, Tang D, Chen J, Hu Y, Cai X, Zhang P. The Clinical Value of GDF15 and Its Prospective Mechanism in Sepsis. Front Immunol. 2021;12:710977. doi: 10.3389/fimmu.2021.710977
31. Dunsmore G, Guo W, Li Z, Bejarano DA, Pai R, Yang K, et al. Timing and location dictate monocyte fate and their transition to tumor-associated macrophages. Sci Immunol. 2024;9(97):eadk3981. doi: 10.1126/sciimmunol.adk3981
32. Ginhoux F, Mulder K, Arcila-Barrera S, Amit I. Embracing macrophage complexity for research and translation. Immunity. 2026;59(11):2885–96. doi: 10.1016/j.immuni.2026.09.015
33. Kzhyshkowska J, Gratchev A, Martens JH, Pervushina O, Mamidi S, Johansson S, et al. Stabilin-1 localizes to endosomes and the trans-Golgi network in human macrophages and interacts with GGA adaptors. J Leukoc Biol. 2004;76(6):1151–61. doi: 10.1189/jlb.0504300
34. Goldman MJ, Craft B, Hastie M, Repecka K, McDade F, Kamath A, et al. Visualizing and interpreting cancer genomics data via the Xena platform. Nat Biotechnol. 2020;38(6):675–8. doi: 10.1038/s41587-020-0546-8
35. Cui H, Zhao G, Lu Y, Zuo S, Duan D, Luo X, et al. TIMER3: an enhanced resource for tumor immune analysis. Nucleic Acids Res. 2025;53(W1):W534–W41. doi: 10.1093/nar/gkaf388
36. Mills KHG. IL-17 and IL-17-producing cells in protection versus pathology. Nat Rev Immunol. 2023;23(1):38–54. doi: 10.1038/s41577-022-00746-9
37. Gowhari Shabgah A, Amir A, Gardanova ZR, Olegovna Zekiy A, Thangavelu L, Ebrahimi Nik M, et al. Interleukin-25: New perspective and state-of-the-art in cancer prognosis and treatment approaches. Cancer Med. 2021;10(15):5191–202. doi: 10.1002/cam4.4060
38. Wong CK, Cheung PF, Ip WK, Lam CW. Interleukin-25-induced chemokines and interleukin-6 release from eosinophils is mediated by p38 mitogen-activated protein kinase, c-Jun N-terminal kinase, and nuclear factor-kappaB. Am J Respir Cell Mol Biol. 2005;33(2):186–94. doi: 10.1165/rcmb.2005-0034OC
39. Letuve S, Lajoie-Kadoch S, Audusseau S, Rothenberg ME, Fiset PO, Ludwig MS, et al. IL-17E upregulates the expression of proinflammatory cytokines in lung fibroblasts. J Allergy Clin Immunol. 2006;117(3):590–6. doi: 10.1016/j.jaci.2005.10.025
40. Bredo G, Storie J, Shrestha Palikhe N, Davidson C, Adams A, Vliagoftis H, et al. Interleukin-25 initiates Th2 differentiation of human CD4(+) T cells and influences expression of its own receptor. Immun Inflamm Dis. 2015;3(4):455–68. doi: 10.1002/iid3.87
41. Bastid J, Dejou C, Docquier A, Bonnefoy N. The Emerging Role of the IL-17B/IL-17RB Pathway in Cancer. Front Immunol. 2020;11:718. doi: 10.3389/fimmu.2020.00718
42. Dai C, Zhang H, Zheng Z, Li CG, Ma M, Gao H, et al. Identification of a distinct cluster of GDF15(high) macrophages induced by in vitro differentiation exhibiting anti-inflammatory activities. Front Immunol. 2024;15:1309739. doi: 10.3389/fimmu.2024.1309739
43. Li M, Song K, Huang X, Fu S, Zeng Q. GDF-15 prevents LPS and D-galactosamine-induced in fl ammation and acute liver injury in mice. Int J Mol Med. 2018;42(3):1756–64. doi: 10.3892/ijmm.2018.3747

44. Lu S, Li R, Deng Y, Bai J, Ji B, Chu Y, et al. GDF15 ameliorates sepsis-induced lung injury via AMPK-mediated inhibition of glycolysis in alveolar macrophage. Respir Res. 2024;25(1):201. doi: 10.1186/s12931-024-02824-z
45. Li R, Wu H, Ran F, He Y, Sun H, Peng W, et al. GDF15 activates the PI3K/AKT pathway to mediate macrophage M2 polarization to promote prostate cancer resistance to docetaxel. Mol Immunol. 2025;185:27–38. doi: 10.1016/j.molimm.2025.07.006
46. Xue J, Schmidt SV, Sander J, Draffehn A, Krebs W, Quester I, et al. Transcriptome-based network analysis reveals a spectrum model of human macrophage activation. Immunity. 2014;40(2):274–88. doi: 10.1016/j.immuni.2014.01.006
47. Kloosterman DJ, Akkari L. Macrophages at the interface of the co-evolving cancer ecosystem. Cell. 2023;186(8):1627–51. doi: 10.1016/j.cell.2023.02.020
48. Matusiak M, Hickey JW, van IDGP, Lu G, Kidzinski L, Zhu S, et al. Spatially Segregated Macrophage Populations Predict Distinct Outcomes in Colon Cancer. Cancer Discov. 2024;14(8):1418–39. doi: 10.1158/2159-8290.CD-23-1300
49. Cheng S, Li Z, Gao R, Xing B, Gao Y, Yang Y, et al. A pan-cancer single-cell transcriptional atlas of tumor infiltrating myeloid cells. Cell. 2021;184(3):792–809 e23. doi: 10.1016/j.cell.2021.01.010
50. Haake M, Haack B, Schafer T, Harter PN, Mattavelli G, Eiring P, et al. Tumor-derived GDF-15 blocks LFA-1 dependent T cell recruitment and suppresses responses to anti-PD-1 treatment. Nat Commun. 2023;14(1):4253. doi: 10.1038/s41467-023-39817-3
51. Furuta S, Jeng YM, Zhou L, Huang L, Kuhn I, Bissell MJ, et al. IL-25 causes apoptosis of IL-25R-expressing breast cancer cells without toxicity to nonmalignant cells. Sci Transl Med. 2011;3(78):78ra31. doi: 10.1126/scitranslmed.3001374
52. Huang CK, Yang CY, Jeng YM, Chen CL, Wu HH, Chang YC, et al. Autocrine/paracrine mechanism of interleukin-17B receptor promotes breast tumorigenesis through NF-kappaB-mediated antiapoptotic pathway. Oncogene. 2014;33(23):2968–77. doi: 10.1038/onc.2013.268
53. Wu HH, Hwang-Verslues WW, Lee WH, Huang CK, Wei PC, Chen CL, et al. Targeting IL-17B-IL-17RB signaling with an anti-IL-17RB antibody blocks pancreatic cancer metastasis by silencing multiple chemokines. J Exp Med. 2015;212(3):333–49. doi: 10.1084/jem.20141702
54. Xu CF, Johnson T, Garcia-Donas J, Choueiri TK, Sternberg CN, Davis ID, et al. IL8 polymorphisms and overall survival in pazopanib- or sunitinib-treated patients with renal cell carcinoma. Br J Cancer. 2015;112(7):1190–8. doi: 10.1038/bjc.2015.64
55. Hess C, Means TK, Autissier P, Woodberry T, Altfeld M, Addo MM, et al. IL-8 responsiveness defines a subset of CD8 T cells poised to kill. Blood. 2004;104(12):3463–71. doi: 10.1182/blood-2004-03-1067
56. Fridman WH, Zitvogel L, Sautes-Fridman C, Kroemer G. The immune contexture in cancer prognosis and treatment. Nat Rev Clin Oncol. 2017;14(12):717–34. doi: 10.1038/nrclinonc.2017.101
57. Zhao C, Wang D, Li Z, Zhang Z, Xu Y, Liu J, et al. IL8 derived from macrophages inhibits CD8(+) T-cell function by downregulating TIM3 expression through IL8-CXCR2 axis in patients with advanced colorectal cancer. Int Immunopharmacol. 2023;121:110457. doi: 10.1016/j.intimp.2023.110457
58. Chen Y, Shen J, Ling C, Liang Z, Huang S, Lin W, et al. Exploring the role of CD8(+) T cells in clear renal cell carcinoma metastasis. FEBS Open Bio. 2024;14(7):1205–17. doi: 10.1002/2211-5463.13819
59. Dong Y, Jiang W, Qiu Y, Xu Z, Cheng J, Ke P, et al. Lactate-Driven IL8+ Tumor-Associated Macrophages Mediate Immunosuppression and Resistance to Immunotherapy in Clear-Cell Renal Cell Carcinoma. Clin Cancer Res. 2026;32(9):1860–73. doi: 10.1158/1078-0432.CCR-25-4384
60. Bilusic M, Heery CR, Collins JM, Donahue RN, Palena C, Madan RA, et al. Phase I trial of HuMax-IL8 (BMS-986253), an anti-IL-8 monoclonal antibody, in patients with metastatic or unresectable solid tumors. J Immunother Cancer. 2019;7(1):240. doi: 10.1186/s40425-019-0706-x

61. Yang D, He Z, Lu J, Yuan X, Liu H, Xue Y, et al. Downregulation of GDF15 suppresses ferroptosis and predicts unfavorable prognosis in clear cell renal cell carcinoma. Cell Div. 2023;18(1):21. doi: 10.1186/s13008-023-00103-9
62. Akdogan O, Ogut B, Sutcuoglu O, Urganci M, Kahya BU, Isik Gonul I, et al. Tumour GDF-15 Expression and Clinical Outcomes in Intermediate-Risk Metastatic Clear-Cell Renal Cell Carcinoma Treated with Second-Line Nivolumab. Curr Oncol. 2026;33(9). doi: 10.3390/curroncol33090531
63. Husaini Y, Qiu MR, Lockwood GP, Luo XW, Shang P, Kuffner T, et al. Macrophage inhibitory cytokine-1 (MIC-1/GDF15) slows cancer development but increases metastases in TRAMP prostate cancer prone mice. PLoS One. 2012;7(8):e43833. doi: 10.1371/journal.pone.0043833
64. Shapouri-Moghaddam A, Mohammadian S, Vazini H, Taghadosi M, Esmaeili SA, Mardani F, et al. Macrophage plasticity, polarization, and function in health and disease. J Cell Physiol. 2018;233(9):6425–40. doi: 10.1002/jcp.26429